FLOCKING BEHAVIORS OF A CUCKER-SMALE ENSEMBLE IN A CYLINDRICAL DOMAIN

HYEONG-OHK BAE*, SEUNG-YEAL HA†, JEONGHO KIM‡, DONGNAM KO§, AND SUNG-IK SOHN¶

Abstract. We study the Cucker-Smale (C-S) type model in a cylindrical domain with a specular reflection boundary condition. When there exist flocking forces along the normal direction to the boundary, then a "*sticky wall*" effect is numerically observed such that particles aggregates in a region nearby the wall of a cylinder. To avoid this sticky wall phenomenon, we adopt a flow-directional flocking force which has no force component normal to the boundary. As a result, we obtain the flocking behavior of particles along the flow direction. Moreover, the emergence of flocking also holds for the corresponding kinetic C-S model. We present a global existence of the classical solution to the kinetic C-S model with the specular reflection boundary condition. In addition, we perform numerical simulations for the particle and kinetic C-S models to demonstrate the aggregation behavior of flocking particles interacting with the boundary.

Key words. Aggregation, alignment, Cucker-Smale model, flocking, specular reflection

AMS subject classifications. 35Q70, 35Q92, 70F10

1. Introduction. Flocking behaviors of self-propelled particles is one of the collective dynamics ubiquitous in our natural, social and artificial complex systems, e.g., the flocking of migratory birds [31, 35, 40], schooling of fish in animal ecology [5, 6, 9, 17], synchronization of oscillators [30, 36, 43], convergence of opinion in social sciences [33] and man-made multi-agent systems in engineering [18, 42], etc. For decades, several mechanical models imitating collective behaviors were proposed in literature [13, 15, 16, 41]. Among them, the Cucker-Smale model [14, 15] is one of the well-studied flocking models in which the velocity of a particle is determined by the weighted average of relative velocities with the other particles. More precisely, let $(x_i, v_i) \in \mathbb{R}^d \times \mathbb{R}^d$ be the position-velocity of the i-th C-S particle. Then, the dynamics of (x_i, v_i) is governed by the Cauchy problem:

$$\begin{cases} \dfrac{dx_i}{dt} = v_i, \quad t > 0, \quad 1 \le i \le N, \\ \dfrac{dv_i}{dt} = \dfrac{\kappa}{N} \displaystyle\sum_{j=1}^{N} \phi(x_i - x_j)(v_j - v_i), \\ (x_i(0), v_i(0)) = (x_{i0}, v_{i0}). \end{cases} \tag{1}$$

Here, κ is a positive constant called the coupling strength, and the function $\phi : \mathbb{R}^d \to \mathbb{R}_+$ is the communication weight which is a nonnegative, radially symmetric bounded

*Department of Financial Engineering, Ajou University, Suwon 16499 Korea (hobae@ajou.ac.kr).

†Department of Mathematical Sciences and Research Institute of Mathematics, Seoul National University, Seoul 08826 Korea, and Korea Institute for Advanced Study, Hoegiro 87, Seoul 02455, Korea (syha@snu.ac.kr).

‡Department of Mathematical Sciences, Seoul National University, Seoul 08826 Korea (jhkim206@snu.ac.kr).

§DeustoTech, University of Deusto, and Facultad de Ingeniería, Universidad de Deusto, Avenida de las Universidades 24, 48007 Bilbao, Bizkaia, Spain (dongnamko@deusto.es).

¶Department of Mathematics, Gangneung-Wonju National University, Gangneung 25457, Korea (sohnsi@gwnu.ac.kr).

function satisfying

$$\begin{aligned} &\phi(x) = \phi(y), \quad \text{if} \quad |x| = |y|, \quad 0 \le \phi(x) \le 1, \ x \in \mathbb{R}^d, \\ &(\phi(x) - \phi(y))(|x| - |y|) \le 0, \quad \forall x, y \in \mathbb{R}^d, \end{aligned} \tag{2}$$

where $|\cdot|$ denotes the standard ℓ^2-norm in $\mathbb{R}^d$. We also define the function $\tilde{\phi} : \mathbb{R}_+ \to \mathbb{R}_+$ as

$$\tilde{\phi}(r) = \phi(x), \quad \text{where} \quad |x| = r.$$

On the other hand, when the number of particles N is sufficiently large, a high-dimensional ODE system (1) can be effectively approximated by the corresponding kinetic equation (3) below. Let $f = f(t, x, v)$ be the one-particle distribution function of a C-S ensemble in the spatial and velocity space $\mathbb{R}^d \times \mathbb{R}^d$ at time t. Then, the dynamics of the kinetic density f is governed by the Cauchy problem to the following Vlasov-type equation:

$$\begin{cases} \partial_t f + v \cdot \nabla_x f + \nabla_v \cdot (F[f]f) = 0, \quad t > 0, \quad (x, v) \in \mathbb{R}^{2d}, \\ F[f](t, x, v) := \kappa \displaystyle\int_{\mathbb{R}^{2d}} \phi(x - x_*)(v_* - v) f(t, x_*, v_*)\, dx_*\, dv_*, \\ f(0, x, v) = f_0(x, v) \ge 0, \quad \displaystyle\int_{\mathbb{R}^{2d}} f_0(x, v)\, dxdv = 1. \end{cases} \tag{3}$$

Then C-S model has been studied from various viewpoints, e.g., asymptotic flocking behavior and mean-field limit [10, 28, 29], macroscopic limit and fluid dynamic description [19, 21, 22, 29, 38], dynamics in stochastic environment [1, 7, 27], bi-cluster problem [11], variants of the C-S model [34, 37], critical coupling strength [25], the first order reduction [23], complete predictability in one-dimensional case [24], uniform mean-field limit [8, 26], flocking of the C-S model with leadership [32, 39], coupled with the either compressible or incompressible fluid [3, 4], etc. For more detailed information about previous results of the C-S model, we refer to a recent survey paper [12]. Although there is extensive literature on the Cauchy problem (1), as far as the authors know, there is no systematic previous work on the initial-boundary value problem on (1) with a physical boundary condition. When the spatial domain Ω is not a whole space $\mathbb{R}^d$ or periodic domain $\mathbb{T}^d$, there should be a physical boundary $\partial\Omega$ with which particles may collide. Then, one may specify an appropriate condition on the velocity after collision. In this paper, we consider the specular reflection boundary condition:

$$v_* = v - 2(n(x) \cdot v)n(x),$$

where v_* is the velocity after collision, and $n(x)$ is the unit normal vector at $x \in \partial\Omega$. Under this framework, we should treat the C-S model (1) in $\Omega \times \mathbb{R}^d$ with the specular reflection boundary condition on $\partial\Omega \times \mathbb{R}^d$. We define the left- and right-sided limits in the following form:

$$v_i(t_*-) := \lim_{t \nearrow t_*} v_i(t) \quad \text{and} \quad v_i(t_*+) := \lim_{t \searrow t_*} v_i(t),$$

where t_* is the time at which the i-th particle collides with the wall. Then, the specular reflection boundary condition is described by

$$v_i(t_*+) = v_i(t_*-) - 2(n(x_i(t_*)) \cdot v_i(t_*-))n(x_i(t_*)), \quad x(t_*) \in \partial\Omega. \tag{4}$$

If there is a flocking force along the normal direction to a boundary, then a strange phenomenon may emerge. More precisely, the ensemble exhibits a sticky property and as a result, particles are hard to escape from the neighborhood of the boundary after collisions. A similar sticky phenomenon near the boundary is numerically observed in the Vicsek model [2]. This phenomenon will be shown analytically in Section 2 for a simple, solvable case, and numerically in Section 6. To avoid this undesired behavior, we introduce a flocking model with the *flow-directional flocking*, which induces the alignment of velocities of particles only along the flow-direction. In this paper, we mainly consider an infinite cylindrical spatial domain:

$$\Omega := \tilde{\Omega} \times \mathbb{R}, \quad \tilde{\Omega} \subset \mathbb{R}^{d-1}, \tag{5}$$

or periodic cylindrical domain:

$$\Omega := \tilde{\Omega} \times \mathbb{T}, \quad \tilde{\Omega} \subset \mathbb{R}^{d-1}, \quad \mathbb{T} := \mathbb{R}/\mathbb{Z}, \tag{6}$$

where $\tilde{\Omega}$ is a compact set. Fig. 1 shows examples of those cylindrical domains. Note that our infinite cylinder is aligned to the direction of the x^d-coordinate in $\mathbb{R}^d$, which coincides with the flow-direction.

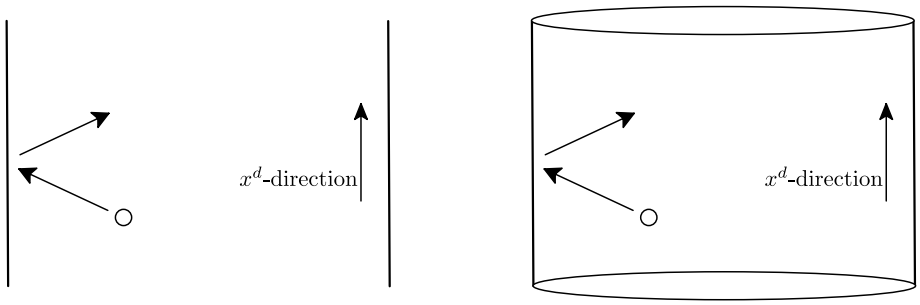

(a) $\Omega = [0,1] \times \mathbb{R}$ (b) $\Omega = \overline{B_1(0)} \times \mathbb{R}$

FIG. 1. *Infinite channel / cylindrical domains*

These typical examples of a domain with boundary are simple, yet interesting from the view point of application, e.g., a flow of particles in a water pipe or blood vessel. Our motivation on the flocking with a boundary is from the application viewpoints, in particular, an alignment of a swarm of robotic sensors which need to check the environment in the pipe. They should not stick to the boundary, while we still expect them to have some kind of ordered behaviors.

With the cylindrical domains, we are able to introduce the C-S model with flow-directional flocking force as follows. Let $(x_i, v_i) \in \Omega \times \mathbb{R}^d$ be the position-velocity of the i-th particle, whose dynamics is governed by the initial-boundary value problem:

$$\begin{cases} \dfrac{dx_i}{dt} = v_i, \quad t > 0, \quad i = 1, \cdots, N, \\ \dfrac{dv_i^k}{dt} = \dfrac{\kappa}{N} \displaystyle\sum_{j=1}^{N} \delta_{kd} \phi(x_i - x_j)(v_j^k - v_i^k), \quad v_i = (v_i^1, \ldots, v_i^d), \\ (x_i(0), v_i(0)) = (x_{i0}, v_{i0}), \\ v_i(t_*+) = v_i(t_*-) - 2(n(x_i(t_*)) \cdot v_i(t_*-))n(x(t_*)), \quad x_i(t_*) \in \partial\Omega. \end{cases} \tag{7}$$

Here, δ_{kd} is the Kronecker delta, which is 1 if $k = d$ and 0 otherwise. This implies that the flocking force in (7) is only acting on velocities in the flow direction, which is x^d-direction. In the model (7), we define the *flow-directional flocking* if and only if the mono-cluster flocking emerges in the direction of flow:

$$\sup_{0\le t<\infty} \max_{i,j} |x_i^d(t) - x_j^d(t)| < \infty \quad \text{and} \quad \lim_{t\to\infty} \max_{i,j} |v_i^d(t) - v_j^d(t)| = 0.$$

Considering the flow-directional flocking model (7), the modified kinetic model corresponds to (3) reads as follows:

$$\begin{cases} \partial_t f + v\cdot\nabla_x f + \nabla_v\cdot(F[f]f) = 0, \\ F[f] = \left(F^1[f], \cdots, F^d[f]\right), \quad (x,v)\in\Omega\times\mathbb{R}^d, \quad t>0, \\ F^k[f](t,x,v) := \kappa\delta_{kd}\displaystyle\int_{\Omega\times\mathbb{R}^d} \phi(x-x_*)(v_*^k - v^k) f(t,x_*,v_*)\,dx_*dv_*, \\ f(0,x,v) = f_0(x,v)\ge 0, \quad x\in\Omega,\ v\in\mathbb{R}^d, \quad \displaystyle\int_{\Omega\times\mathbb{R}^d} f_0(x,v)\,dxdv = 1, \\ f(t,x,v) = f(t,x,v-2(n(x)\cdot v)n(x)), \quad x\in\partial\Omega, \quad v\cdot n(x)\le 0. \end{cases} \tag{8}$$

The main results of this paper is two-fold. First, we analyze the emergent dynamics of the flocking model (7) and its kinetic model (8) to obtain flow-directional flocking results by providing sufficient conditions in terms of initial data, coupling strength and communication weight. As shown for the two-particle analysis in Section 2, a portion of C-S ensemble will aggregate near the boundary (a *sticky wall phenomenon*). To avoid this kind of singular behavior of the ensemble, we only turn on the flocking force in the flow-direction and turn it off in other directions. Thus, in general, the whole ensemble does not exhibit flocking behaviors as in the C-S model [15, 28, 29], however, we can see that the flow-directional component of the velocities (in our setting, x^d-coordinate) exhibits a nice flocking behavior. We provide sufficient conditions leading to the flow-directional flocking for the particle model (7) and the kinetic model (8) (see Theorem 3.2 for the particle model and Theorem 4.2 and Theorem 4.4 for the kinetic model). Second, we study a global unique solvability of the kinetic model (8) in a Hölder space by using the successive approximations and studying the propagation of Hölder-regularity along the bi-characteristics.

The rest of the paper is organized as follows. In Section 2, we briefly discuss a motivation of the flow-directional flocking model and its basic properties. In Section 3, we study a flocking estimate for (7). In Section 4, we present the kinetic model of (7), and analyze its flocking behavior as well. In Section 5, we establish a global existence and uniqueness of the classical solution to the kinetic model proposed in Section 4. In Section 6, we perform several numerical simulations of the particle and kinetic models. Finally, Section 7 is devoted to a brief summary of our main results.

2. Preliminaries.

In this section, we present several properties of the C-S model with the specular reflection boundary condition such as a motivation for the flow-directional flocking force and conservation laws.

2.1. A motivation for flow-directional flocking.

In this subsection, we provide a motivation for introducing the flow-directional flocking force instead of the original flocking force. We consider a simple setting of the two-particle system on

a line segment. Suppose that the spatial domain Ω is $[0, 10]$ and the initial data $(x_{10}, x_{20}, v_{10}, v_{20})$ are given by

$$x_{10} = 1, \quad x_{20} = 2, \quad v_{10} = -1, \quad v_{20} = -1.$$

For simplicity, we assume that the communication weight ϕ is constant:

$$\phi(x) \equiv \phi_0.$$

Now, we consider the original flocking model (1). Then, the dynamics of this two-particle C-S system is governed by the following system:

$$\frac{dv_1}{dt} = \frac{\kappa}{2}\phi_0(v_2 - v_1), \quad \frac{dv_2}{dt} = \frac{\kappa}{2}\phi_0(v_1 - v_2), \quad t > 0, \tag{9}$$

subject to the specular reflection boundary condition (4). Since their initial velocities are identical, there is no force applied to both particles. Hence, the particles will maintain their dynamics until x_1 collides with the boundary, $x_1(t) = 0$ at $t = 1$. Since we consider the specular reflection boundary condition,

$$v_1(1+) = -v_1(1-) = 1.$$

Next, we consider the dynamics of $t > 1$. Let $t = t_*$ be the next collision time between the particles and boundary, where $x_2(t_*) = 0$ or $x_1(t_*) = 10$. If there is no collision after $t = 1$, we let $t_* = \infty$. Then, for $t \in (1, t_*)$, we can take the quantitative analysis. First, we have the symmetry of two particles to get

$$\frac{d}{dt}(v_1 + v_2) = 0 \quad \text{so that} \quad v_1(t) + v_2(t) = v_1(1+) + v_2(1) = 0, \quad \text{for } \ t \in (1, t_*).$$

This implies that the sum of two positions is also conserved:

$$\frac{d}{dt}(x_1 + x_2) = 0 \quad \text{so that} \quad x_1(t) + x_2(t) = 1, \quad \text{for } \ t \in (1, t_*).$$

Hence if $t_* < \infty$, then the collision occurs when x_2 hits 0 and we have

$$x_1(t_*) = 1 \quad \text{and} \quad x_2(t_*) = 0. \tag{10}$$

On the other hand, we take a difference between two velocities (9) to obtain

$$\frac{d(v_1 - v_2)}{dt} = -\kappa\phi_0(v_1 - v_2), \quad \text{for } \ t \in (1, t_*). \tag{11}$$

This gives the exponential flocking:

$$v_1(t) - v_2(t) = (v_1(1+) - v_2(1))e^{-\kappa\phi_0 t} = 2e^{-\kappa\phi_0 t}.$$

Note that the maximal velocity $\max\{|v_1|, |v_2|\}$ is decreasing. We now integrate (11) to get the position difference for $t \in (1, t_*)$:

$$x_1(t) - x_2(t) = x_1(1) - x_2(1) + \int_1^t 2e^{-\kappa\phi_0 s}\, ds = -1 + \frac{2}{\kappa\phi_0}\left(1 - e^{-\kappa\phi_0 t}\right). \tag{12}$$

Suppose that $\kappa\phi_0 > 1$. Then, for $t \in (1, t_*)$,

$$\begin{aligned} x_1(t) - x_2(t) &= -1 + \frac{2}{\kappa\phi_0}\left(1 - e^{-\kappa\phi_0 t}\right) \le -1 + 2\left(1 - e^{-\kappa\phi_0 t}\right) \\ &= 1 - 2e^{-\kappa\phi_0 t} < 1. \end{aligned} \tag{13}$$

If there is a collision of x_2 with the boundary point 0 at a finite time $t_* < \infty$, then (10) implies that

$$x_1(t_*) = 1, \quad x_2(t_*) = 0, \quad \text{and hence} \quad x_1(t_*) - x_2(t_*) = 1. \tag{14}$$

Hence, (10) contradicts the dynamics (13) since the trajectories are continuous. This shows that there is no collision of x_2 to the boundary 0 and $t_* = \infty$. We have the following convergence of positions:

$$\lim_{t\to\infty} x_1(t) = \frac{1}{\kappa\phi_0}, \quad \lim_{t\to\infty} x_2(t) = 1 - \frac{1}{\kappa\phi_0}.$$

Therefore, when the flocking force is applied to the particles along the normal direction to the boundary, there is a possibility that the particles aggregate near the boundary. Even if we have a smaller coupling strength, $\kappa\phi_0 < 1$, two particles will have their third collision at the boundary $x = 10$ with a smaller speed and the same position difference. In fact, it follows from (12) and (14) that the second collision time is $t_* = -\frac{\log(1-\kappa\phi_0)}{\kappa\phi_0}$, and since $v_1(t) + v_2(t) = 0$ for $t \in (1, t_*)$, we have

$$v_1(t_*) = v_2(t_*+) = -v_2(t_*-) = e^{-\kappa\phi_0 t_*} \quad \text{and} \quad x_1(t_*) - x_2(t_*) = 1.$$

Therefore, eventually, two particles will converge to the position somewhere in $[0, 1] \cup [9, 10]$.

This "sticky wall" phenomenon is also observed numerically in the N-body C-S dynamics with a general communication weight in Section 6. Heuristically, this phenomenon is due to the interaction between the particles coming out from the boundary and going into the boundary. Although this phenomenon has an interesting aspect, it seems not so beneficial both in analytic and applicational points of view. The sticky phenomenon itself makes the analysis much harder, and when we consider possible applications such as swarming robots in a pipe or blood vessel, sticking to the boundary can make particles difficult to reach to the target. Therefore, we introduce the flocking model (7) which does not have flocking forces normal to the boundary.

2.2. Conservation laws. In this subsection, we present conservation laws for the C-S model with boundary (7). Unlike the C-S model (1) on the whole space, there is no general conservation of the total momentum due to the discontinuity in velocities from the specular reflection at the boundary. However, there are still conservation laws along the flow direction.

LEMMA 2.1. *Let $\{(x_i, v_i)\}$ be a solution to (7) with initial data $\{(x_{i0}, v_{i0})\}$. Then, we have*

$$\frac{d}{dt}\left(\sum_{i=1}^N v_i^d\right) = 0 \quad \textit{and} \quad \frac{d}{dt}\left(\sum_{i=1}^N x_i^d - t\sum_{i=1}^N v_{i0}^d\right) = 0.$$

Proof. The proof is essentially the same as the Cucker-Smale model. More precisely, we use the index-changing trick to get

$$\frac{d}{dt}\left(\sum_{i=1}^N v_i^d\right) = \frac{\kappa}{N}\sum_{i,j=1}^N \phi(x_i - x_j)(v_j^d - v_i^d) = 0.$$

Then, the second equation directly follows from the first equation of (7). ∎

REMARK 2.2. *Due to the presence of a boundary, system (7) is not Galilean invariant. However, it is Galilean invariant along the x^d- and v^d-coordinates. By the conservation laws in Lemma 2.1, we may assume*

$$\sum_{i=1}^N v_i^d = 0, \quad \sum_{i=1}^N x_i^d(t) = \sum_{i=1}^N x_{i0}^d.$$

Under these assumptions, the flow-directional flocking can be stated as follows,

$$\sup_{0\le t<\infty} |x_i^d(t)| < \infty \quad \textit{and} \quad \lim_{t\to\infty} |v_i^d(t)| = 0, \quad i = 1, 2, \dots, N.$$

3. Emergence of flow-directional flocking for a particle model. In this section, we present the flow-directional flocking result of the model (7). For this, we first define the position and velocity diameters:

$$D_x^d(t) := \max_{1\le i,j\le N} |x_i^d(t) - x_j^d(t)|, \quad D_v^d(t) := \max_{1\le i,j\le N} |v_i^d(t) - v_j^d(t)|.$$

Then, we derive a system of dissipative differential inequalities for $D_x^d(t)$ and $D_v^d(t)$ in the following lemma.

LEMMA 3.1. *Let $\{(x_i, v_i)\}$ be a solution to (7) with initial data $\{(x_{i0}, v_{i0})\}$ satisfying*

$$\sum_{i=1}^N v_{i0}^d = 0.$$

Then, D_x^d and D_v^d satisfy the following differential inequalities:

$$\left|\frac{d}{dt} D_x^d\right| \le D_v^d, \qquad \frac{d}{dt} D_v^d \le -\kappa\tilde{\phi}\left(D(\tilde{\Omega}) + D_x^d\right) D_v^d, \quad \textit{a.e. } t > 0,$$

where $D(\tilde{\Omega})$ is the diameter of a compact region $\tilde{\Omega}$ in $\mathbb{R}^{d-1}$ (see (5) and (6)).

Proof. Since the first inequality is almost trivial, we focus on the second differential inequality. We basically follow the same arguments in the proof of Lemma 2.2 in [26]. First, we define auxiliary functions $\Phi_{ij}(t)$ as

$$\Phi_{ij}(t) := \frac{\phi(x_i - x_j)}{N} + \left(1 - \frac{\sum_{j=1}^N \phi(x_i - x_j)}{N}\right)\delta_{ij},$$

where δ_{ij} is the Kronecker delta. Then, it is easy to see that Φ_{ij} satisfies

$$\Phi_{ij} \ge \frac{\phi(x_i - x_j)}{N}, \quad \sum_{k=1}^N \Phi_{ik} = 1, \quad \sum_{k=1}^N \Phi_{ik}(v_k^d - v_i^d) = \sum_{k=1}^N \frac{\phi(x_i - x_k)}{N}(v_k^d - v_i^d).$$

Next, we choose the maximal and minimal indices M and m such that

$$v_M^d := \max_{1\le i\le N} v_i^d, \quad v_m^d := \min_{1\le i\le N} v_i^d, \quad v_M^d - v_m^d = D_v^d.$$

Then, we have

$$
\begin{aligned}
&\frac{1}{2}\frac{d}{dt}(v_M^d - v_m^d)^2 \\
&\quad = \kappa(v_M^d - v_m^d)\left[\sum_{j=1}^N \frac{\phi(x_M - x_j)}{N}(v_j^d - v_M^d) - \sum_{j=1}^N \frac{\phi(x_m - x_j)}{N}(v_j^d - v_m^d)\right] \\
&\quad = \kappa(v_M^d - v_m^d)\left[\sum_{j=1}^N \Phi_{Mj}(v_j^d - v_M^d) - \sum_{j=1}^N \Phi_{mj}(v_j^d - v_m^d)\right] \\
&\quad = -\kappa(v_M^d - v_m^d)^2 + \kappa(v_M^d - v_m^d)\left[\sum_{j=1}^N (\Phi_{Mj} - \Phi_{mj})\, v_j^d\right] \\
&\quad = -\kappa(v_M^d - v_m^d)^2 + \kappa(v_M^d - v_m^d)\left[\sum_{j=1}^N (\Phi_{Mj} - \min\{\Phi_{Mj}, \Phi_{mj}\})\, v_j^d\right] \\
&\qquad - \kappa(v_M^d - v_m^d)\left[\sum_{j=1}^N (\Phi_{mj} - \min\{\Phi_{Mj}, \Phi_{mj}\})\, v_j^d\right].
\end{aligned} \tag{15}
$$

On the other hand, it follows from definitions of extremal indices that

$$
(v_M^d - v_m^d)v_m^d \le (v_M^d - v_m^d)v_j^d \le (v_M^d - v_m^d)v_M^d, \quad 1 \le j \le N. \tag{16}
$$

In (15), we use (16) to obtain,

$$
\begin{aligned}
\frac{1}{2}\frac{d}{dt}(v_M^d - v_m^d)^2 &\le -\kappa(v_M^d - v_m^d)^2 + \kappa(v_M^d - v_m^d)\left[\sum_{j=1}^N (\Phi_{Mj} - \min\{\Phi_{Mj}, \Phi_{mj}\})\, v_M^d\right] \\
&\quad - \kappa(v_M^d - v_m^d)\left[\sum_{j=1}^N (\Phi_{mj} - \min\{\Phi_{Mj}, \Phi_{mj}\})\, v_m^d\right] \\
&= -\kappa(v_M^d - v_m^d)^2 + \kappa(v_M^d - v_m^d)v_M^d - \kappa(v_M^d - v_m^d)v_m^d \\
&\quad -\kappa(v_M^d - v_m^d)^2 \sum_{j=1}^N \min\{\Phi_{Mj}, \Phi_{mj}\} \quad \left(\because \sum_{k=1}^N \Phi_{ik} = 1\right) \\
&= -\kappa(v_M^d - v_m^d)^2 \sum_{j=1}^N \min\{\Phi_{Mj}, \Phi_{mj}\} \le -\kappa\tilde{\phi}(D_x(t))\left|v_M^d - v_m^d\right|^2,
\end{aligned}
$$

where $D_x(t) := \max\limits_{1\le i,j\le N} |x_i(t) - x_j(t)|$.

Then, it follows from the triangle inequality that

$$
|x_i(t) - x_j(t)| \le \sum_{k=1}^d \left|x_i^k(t) - x_j^k(t)\right| \le D(\tilde{\Omega}) + \left|x_i^d(t) - x_j^d(t)\right| \le D(\tilde{\Omega}) + D_x^d(t),
$$

where $D(\tilde{\Omega})$ is the diameter of the compact set $\tilde{\Omega}$. Hence, we have

$$
D_x(t) \le D(\tilde{\Omega}) + D_x^d(t),
$$

and thus,

$$\frac{1}{2}\frac{d}{dt}\left|v_M^d - v_m^d\right|^2 \le -\kappa\tilde{\phi}\left(D(\tilde{\Omega}) + D_x^d\right)\left|v_M^d - v_m^d\right|^2. \qquad \square$$

Now, we are ready to prove the flow-directional flocking of (7).

THEOREM 3.2. *Suppose that the initial data, coupling strength and communication weight satisfy*

$$\sum_{i=1}^{N} v_{i0}^d = 0, \quad \textit{and} \quad D_v^d(0) < \kappa\int_{D(\tilde{\Omega})+D_x^d(0)}^{\infty}\tilde{\phi}(s)\,ds,$$

where $D(\tilde{\Omega})$ is the diameter of $\tilde{\Omega}$, and let (x_i, v_i) be a solution to (7). Then, there exist a positive constant x_d^∞ such that

$$\sup_{0\le t<\infty} D_x^d(t) \le x_d^\infty, \quad D_v^d(t) \le D_v^d(0)e^{-\kappa\tilde{\phi}\left(x_d^\infty + D(\tilde{\Omega})\right)t}, \quad t > 0.$$

Proof. From Lemma 3.1, one has

$$\left|\frac{d}{dt}D_x^d\right| \le D_v^d, \quad \frac{d}{dt}D_v^d \le -\kappa\tilde{\phi}\left(D(\tilde{\Omega}) + D_x^d\right)D_v^d, \quad t > 0.$$

Using these differential inequalities, we adopt the Lyapunov functional approach in [28]. Suppose that the initial data, coupling strength and communication weight satisfy

$$D_v^d(0) < \kappa\int_{D(\tilde{\Omega})+D_x^d(0)}^{\infty}\tilde{\phi}(s)\,ds,$$

then there exist a constant $\mathcal{X}$ such that

$$\sup_{0\le t<\infty}\left(D(\tilde{\Omega}) + D_x^d\right) \le \mathcal{X}, \quad D_v^d(t) \le D_v^d(0)e^{-\kappa\tilde{\phi}(\mathcal{X})t}, \quad t > 0.$$

Therefore, we take $x_d^\infty := \mathcal{X} - D(\tilde{\Omega})$ to obtain the desired estimate. For details, we refer to [28]. $\square$

4. Emergence of flow-directional flocking for a kinetic model. In this section, we present the flow-directional flocking estimates of the kinetic C-S model with a boundary. As in the C-S model, we consider the modified C-S kinetic model whose flocking force is applied along the flow direction, in our case, the x^d–coordinate only. Then, the dynamics of the kinetic density f is governed by the initial-boundary problem for the kinetic model (8):

$$\begin{cases} \partial_t f + v\cdot\nabla_x f + \nabla_v\cdot(F[f]f) = 0, \\ F[f] = \left(F^1[f], \cdots, F^d[f]\right), \quad (x,v)\in\Omega\times\mathbb{R}^d, \quad t > 0, \\ F^k[f](t,x,v) := \kappa\delta_{kd}\displaystyle\int_{\Omega\times\mathbb{R}^d}\phi(x-x_*)(v_*^k - v^k)f(t,x_*,v_*)\,dx_*dv_*, \\ f(0,x,v) = f_0(x,v) \ge 0, \quad x\in\Omega,\ v\in\mathbb{R}^d, \quad \displaystyle\int_{\Omega\times\mathbb{R}^d} f_0(x,v)\,dxdv = 1, \\ f(t,x,v) = f(t,x,v-2(n(x)\cdot v)n(x)), \quad x\in\partial\Omega, \quad v\cdot n(x)\le 0. \end{cases}$$

The global existence of a classical solution to (8) will be given in Section 5, and in the sequel, we will mainly focus on the emergence of flow-directional flocking on

two distinct domains, an infinite cylinder $\Omega = \tilde{\Omega} \times \mathbb{R}$ and periodic cylinder $\Omega = \tilde{\Omega} \times \mathbb{T}$, $\mathbb{T} := \mathbb{R}/\mathbb{Z}$. Before we move to flocking estimates, we recall conservation laws associated with (8).

LEMMA 4.1. *Let f be a classical solution to (8). Then, we have the following conservation laws:*

1. *The total mass is conserved:*
$$\int_{\Omega\times\mathbb{R}^d} f(t,x,v)\,dxdv = \int_{\Omega\times\mathbb{R}^d} f_0(x,v)\,dxdv.$$
2. *The d-component of the total momentum is conserved:*
$$\int_{\Omega\times\mathbb{R}^d} v^d f(t,x,v)\,dxdv = \int_{\Omega\times\mathbb{R}^d} v^d f_0(x,v)\,dxdv.$$

Proof. (1) Note that the following term
$$\int_{\Omega\times\mathbb{R}^d} \nabla_v\cdot(F[f]f)\,dx\,dv = \int_\Omega \left(\int_{\mathbb{R}^d} \nabla_v\cdot(F[f]f)\,dv\right) dx$$
vanishes since the velocity domain is the whole space $\mathbb{R}^d$. Thus, we have
$$\frac{d}{dt}\int_{\Omega\times\mathbb{R}^d} f(t,x,v)\,dxdv = -\int_{\Omega\times\mathbb{R}^d} v\cdot\nabla_x f(t,x,v)\,dxdv.$$
Since
$$\int_{\Omega\times\mathbb{R}^d} v^d\partial_{x^d} f\,dxdv = 0,$$
we only consider the integral over $\tilde{\Omega}$ and its tangent space:
$$\int_{\tilde{\Omega}\times\mathbb{R}^{d-1}} \tilde{v}\cdot\nabla_{\tilde{x}} f(t,x,v)\,d\tilde{x}d\tilde{v},$$
where $x = (\tilde{x}, x^d)$ and $v = (\tilde{v}, v^d)$.

The divergence theorem yields
$$\int_{\tilde{\Omega}} \tilde{v}\cdot\nabla_{\tilde{x}} f(t,x,v)\,d\tilde{x} = \int_{\partial\tilde{\Omega}} \tilde{v}\cdot\tilde{n} f(t,x,v)\,dS,$$
and thus,
$$\int_{\tilde{\Omega}\times\mathbb{R}^{d-1}} \tilde{v}\cdot\nabla_{\tilde{x}} f(t,x,v)\,d\tilde{x}d\tilde{v} = \int_{\partial\tilde{\Omega}\times\mathbb{R}^{d-1}} \tilde{v}\cdot\tilde{n} f(t,x,v)\,dS\,d\tilde{v}.$$
We now use change of variable $\tilde{w} = \tilde{v} - 2(\tilde{n}\cdot\tilde{v})\tilde{n}$ to obtain for $\tilde{x}\in\partial\tilde{\Omega}$
$$\begin{aligned}
&\int_{\mathbb{R}^{d-1}} \tilde{v}\cdot\tilde{n} f\left(\tilde{x}, x^d, \tilde{v}, v^d\right)\,d\tilde{v}\\
&= \int_{\{\tilde{v}\,:\,\tilde{n}\cdot\tilde{v}>0\}} \tilde{v}\cdot\tilde{n} f\left(\tilde{x}, x^d, \tilde{v}, v^d\right)\,d\tilde{v} + \int_{\{\tilde{v}\,:\,\tilde{n}\cdot\tilde{v}<0\}} \tilde{v}\cdot\tilde{n} f\left(\tilde{x}, x^d, \tilde{v}, v^d\right)\,d\tilde{v}\\
&= \int_{\{\tilde{v}\,:\,\tilde{n}\cdot\tilde{v}>0\}} \tilde{v}\cdot\tilde{n} f\left(\tilde{x}, x^d, \tilde{v}, v^d\right)\,d\tilde{v} + \int_{\{\tilde{v}\,:\,\tilde{n}\cdot\tilde{v}<0\}} \tilde{v}\cdot\tilde{n} f\left(\tilde{x}, x^d, \tilde{v}-2(\tilde{n}\cdot\tilde{v})\tilde{n}, v^d\right)\,d\tilde{v}\\
&= \int_{\{\tilde{v}\,:\,\tilde{n}\cdot\tilde{v}>0\}} \tilde{v}\cdot\tilde{n} f\left(\tilde{x}, x^d, \tilde{v}, v^d\right)\,d\tilde{v} - \int_{\{\tilde{w}\,:\,\tilde{n}\cdot\tilde{w}>0\}} \tilde{w}\cdot\tilde{n} f\left(\tilde{x}, x^d, \tilde{w}, v^d\right)\,d\tilde{w} = 0.
\end{aligned}$$

Therefore, we have the conservation of mass:

$$\frac{d}{dt}\int_{\Omega\times\mathbb{R}^d} f(t,x,v)\,dxdv = 0.$$

(2) We need to show that the specular reflection boundary condition in (8) does not affect the d-component of the momentum. For this, we use (8) to get

$$\begin{aligned}\frac{d}{dt}&\int_{\Omega\times\mathbb{R}^d} v^d f(t,x,v)\,dxdv \\ &= -\int_{\Omega\times\mathbb{R}^d} v^d (v\cdot\nabla_x f(t,x,v))\,dxdv - \int_{\Omega\times\mathbb{R}^d} v^d \partial_{v^d}(F^d[f]f)\,dxdv.\end{aligned} \tag{17}$$

The first term on the right-hand side of (17) vanishes as in the proof of (1), whereas for the second term, we use the integration by parts to obtain

$$\begin{aligned}-\int_{\Omega\times\mathbb{R}^d} v^d\partial_{v^d}(F^d[f]f)\,dxdv &= \int_{\Omega\times\mathbb{R}^d} F^d[f]f\,dxdv \\ &= \int_{(\Omega\times\mathbb{R}^d)^2} \phi(x-x_*)(v_*^d - v^d) f(t,x,v) f(t,x_*,v_*)\,dxdv\,dx_*dv_* = 0.\end{aligned}$$

Therefore, one has the conservation law for d-component of total momentum:

$$\frac{d}{dt}\int_{\Omega\times\mathbb{R}^d} v^d f(t,x,v)\,dxdv = 0.$$

□

Without loss of generality, as in the C-S model in Section 3, we assume that the d-th component of the total momentum is initially zero. Moreover, we also assume that the initial datum has the unit mass. Then, we have

$$\int_{\Omega\times\mathbb{R}^d} v^d f(t,x,v)\,dxdv = 0, \quad \int_{\Omega\times\mathbb{R}^d} f(t,x,v)\,dxdv = 1.$$

4.1. Flocking in an infinite cylinder. In this subsection, we present the flocking estimate in an infinite cylinder. We will use similar arguments as in Section 3, which uses piecewise continuous characteristic curves. More precisely, we consider the characteristic curves defined as a solution to the following system:

$$\begin{aligned}&\frac{dx(s)}{ds} = v(s), \quad v(s) = \left(v^1(s),\cdots,v^d(s)\right), \quad t_1 \le s \le t_2, \\ &\frac{dv^k(s)}{ds} = \kappa\delta_{kd}\int_{\Omega\times\mathbb{R}^d} \phi(x-x_*)\left(v_*^k - v^k(s)\right) f(t,x_*,v_*)\,dx_*\,dv_*,\end{aligned} \tag{18}$$

where the interval (t_1,t_2) lies between two consecutive collisions with a boundary. Since we can only expect flocking behavior along the x^d-coordinate, we define diameters of the support of f projected on x^d- and v^d-coordinates as follows:

$$\begin{aligned}D_x^d(f(t)) &:= \sup_{x^d} \mathrm{supp}_{x_d} f(t,\cdot,\cdot) - \inf_{x^d} \mathrm{supp}_{x_d} f(t,\cdot,\cdot), \\ D_v^d(f(t)) &:= \sup_{v^d} \mathrm{supp}_{v_d} f(t,\cdot,\cdot) - \inf_{v^d} \mathrm{supp}_{v_d} f(t,\cdot,\cdot).\end{aligned} \tag{19}$$

Of course, the intuition behind this definition is originated from Lemma 3.1. Since it is clear that

$$\left|\frac{dD_x^d(f(t))}{dt}\right| \le D_v^d(f(t)), \tag{20}$$

we focus on the derivation of the differential inequality on $D_v^d(f(t))$, parallel to Lemma 3.1. Let $(x_M(s), v_M(s))$ and $(x_m(s), v_m(s))$ be the two characteristic curves corresponding to the maximum and minimum trajectories of v^d, respectively. In other words,

$$v_M^d(s) := \sup \mathrm{supp}_{v^d} f(s), \quad v_m^d(s) := \inf \mathrm{supp}_{v^d} f(s), \quad v_M^d(s) - v_m^d(s) = D_v^d(f(s)).$$

Moreover, we set $f_* := f(s, x_*, v_*)$ and denote the diameter of $\tilde{\Omega}$ by $D(\tilde{\Omega})$. Since the characteristic curves for maximum and minimum velocity are piecewise Lipschitz continuous, we may use (18) for these maximum and minimum velocities for a.e. t. Thus, we have

$$\begin{aligned}\frac{dv_M^d(s)}{ds} &= \kappa \int_{\Omega\times\mathbb{R}^d} \phi(x_M(s) - x_*)\left(v_*^d - v_M^d(s)\right) f_*\, dx_*\, dv_* \\ &\le \kappa\tilde{\phi}\left(D(\tilde{\Omega}) + D_x^d(f(s))\right)\int_{\Omega\times\mathbb{R}^d}\left(v_*^d - v_M^d(s)\right) f_*\, dx_*\, dv_*,\end{aligned}$$

and similarly,

$$\begin{aligned}\frac{dv_m^d(s)}{ds} &= \kappa \int_{\Omega\times\mathbb{R}^d} \phi(x_m(s) - x_*)\left(v_*^d - v_m^d(s)\right) f_*\, dx_*\, dv_* \\ &\ge \kappa\tilde{\phi}\left(D(\tilde{\Omega}) + D_x^d(f(s))\right)\int_{\Omega\times\mathbb{R}^d}(v_*^d - v_m^d(s)) f_*\, dx_*\, dv_*.\end{aligned}$$

Therefore, we get

$$\begin{aligned}\frac{d\left(v_M^d - v_m^d\right)}{ds} &\le \kappa\tilde{\phi}\left(D(\tilde{\Omega}) + D_x^d(f(s))\right)\left(v_m^d(s) - v_M^d(s)\right)\int_{\Omega\times\mathbb{R}^d} f_*\, dx_*\, dv_* \\ &= -\kappa\tilde{\phi}\left(D(\tilde{\Omega}) + D_x^d(f(s))\right)\left(v_M^d(s) - v_m^d(s)\right).\end{aligned}$$

Here the last inequality is due to the mass conservation law. This implies

$$\frac{dD_v^d(f(t))}{dt} \le -\kappa\tilde{\phi}\left(D(\tilde{\Omega}) + D_x^d(f(t))\right) D_v^d(f(t)). \tag{21}$$

The above inequality together with (20) yields exactly the same differential inequalities as in Lemma 3.1. Therefore, we can apply the same argument in Theorem 3.2 to obtain the following flocking theorem for the kinetic model as below.

THEOREM 4.2. *Suppose that the initial datum, coupling strength and communication weight satisfy*

$$\int_{\Omega\times\mathbb{R}^d} v^d f_0(x,v)\, dxdv = 0, \quad D_v^d(f_0) < \kappa\int_{D(\tilde{\Omega})+D_x^d(f_0)}^{\infty}\tilde{\phi}(s)\, ds,$$

and let f be a solution to (8). Then, there exist a positive constant x_d^∞ such that

$$\sup_{0\le t<\infty} D_x^d(f(t)) \le x_d^\infty, \quad D_v^d(f(t)) \le D_v^d(f_0)e^{-\kappa\tilde{\phi}\left(x_d^\infty + D(\tilde{\Omega})\right)t}, \quad t > 0.$$

REMARK 4.3.

1. *In fact, guaranteeing the maximal characteristic curve* $(x_M(s), v_M(s))$ *and justification of* (21) *are not trivial matters. More precisely, there may be infinite number of collisions within a finite-time interval to the maximum velocity. In order to obtain the estimation* (21) *rigorously, we may follow the idea in [10, Section 4] in which the authors approximate the particle distribution* f *by empirical measures to obtain the estimate on the velocity support.*

2. *From the differential inequality*

$$\frac{dD_v^d(f(t))}{dt} \le -\kappa\tilde{\phi}\left(D(\tilde{\Omega}) + D_x^d(f(t))\right) D_v^d(f(t)) \le 0,$$

we obtain the uniform boundedness of the velocity support. This directly comes from the fact that there is no flocking force applied to other velocity coordinate. To sum up, we have

$$\sup_{v\in \mathrm{supp} f(t)} |v| \le \sup_{v\in \mathrm{supp} f_0} |v|.$$

This also implies the boundedness of spatial support of f *up to any finite time* T*.*

4.2. Flocking in a periodic cylinder. In this subsection, we consider a periodic cylinder for the spatial domain. Since the spatial domain is already bounded, we can define the smallest positive communication weight:

$$\phi_m := \min_{x,x_*\in\Omega} \phi(x - x_*) > 0.$$

From this fact, we can obtain a unconditional flocking estimate. Again, we will use a Lyapunov functional approach for simpler estimates, although we may use the same argument as in Section 4.1. First, we define the partial kinetic energy $\mathcal{E}_d$:

$$\mathcal{E}_d(t) := \int_{\Omega\times\mathbb{R}^d} \left|v^d\right|^2 f(t,x,v)\,dxdv. \tag{22}$$

THEOREM 4.4. *Suppose that the spatial domain* $\Omega = \tilde{\Omega}\times\mathbb{T}$*, and let* f *be a solution to* (8)*. Then, one has*

$$\mathcal{E}_d(t) \le \mathcal{E}_d(0)e^{-2\kappa\phi_m t}, \quad t \ge 0.$$

Proof. We set $x = (\tilde{x}, x^d)$ and $v = (\tilde{v}, v^d)$, then note that the integration over x^d and v has no boundary values. We now use the integration by parts to yield

$$\begin{aligned}
\frac{d\mathcal{E}_d}{dt} &= \int_{\Omega\times\mathbb{R}^d} \left|v^d\right|^2 \left(-v\cdot\nabla_x f - \nabla_v\cdot(F[f]f)\right) dxdv \\
&= -\int_{\Omega\times\mathbb{R}^d} \nabla_{\tilde{x}}\cdot\left(\left|v^d\right|^2\tilde{v}f\right) dxdv - \int_{\Omega\times\mathbb{R}^d} \left|v^d\right|^2 \partial_{v^d}F^d[f]f\,dxdv \\
&= -\int_{\Omega\times\mathbb{R}^d} \nabla_{\tilde{x}}\cdot\left(\left|v^d\right|^2\tilde{v}f\right) dxdv + 2\int_{\Omega\times\mathbb{R}^d} v^d F^d[f]f\,dxdv \\
&=: \mathcal{I}_{11} + \mathcal{I}_{12}.
\end{aligned}$$

Below, we estimate the terms $\mathcal{I}_{1i}$, $i = 1, 2$, separately.

• (Estimate of $\mathcal{I}_{11}$) : We use the divergence theorem on the integral over $\tilde{\Omega}$ to obtain

$$\int_{\tilde{\Omega}} \nabla_{\tilde{x}} \cdot \left(\left|v^d\right|^2 \tilde{v} f \right) d\tilde{x} = \int_{\partial\tilde{\Omega}} \left|v^d\right|^2 \tilde{v} \cdot \tilde{n} f(x,v)\, dS,$$

where $\Omega = \tilde{\Omega} \times \mathbb{T}$. Then, we use the specular reflection boundary conditions to find

$$\int_{\tilde{\Omega}\times\mathbb{R}^{d-1}} \nabla_{\tilde{x}} \cdot \left(\left|v^d\right|^2 \tilde{v} f \right) d\tilde{x} d\tilde{v} = \left|v^d\right|^2 \int_{\mathbb{R}^{d-1}} \int_{\partial\tilde{\Omega}} \tilde{v} \cdot \tilde{n} f \left(\tilde{x}, x^d, \tilde{v}, v^d\right) dS\, d\tilde{v} = 0,$$

where we used the same argument as in Lemma 4.1. Hence, we have

$$\mathcal{I}_{11} = 0.$$

• (Estimate of $\mathcal{I}_{12}$) : We use definition of F^d and set $f_* := f(t, x_*, v_*)$ to obtain

$$\begin{aligned}
\mathcal{I}_{12} &= 2\kappa \int_{\Omega\times\mathbb{R}^d} \phi(x - x_*) v^d \big(v_*^d - v^d\big) f f_*\, dx_*\, dv_*\, dx dv \\
&= -\kappa \int_{\Omega\times\mathbb{R}^d} \phi(x - x_*) \left|v^d - v_*^d\right|^2 f f_*\, dx dv\, dx_* dv_* \\
&\le -\kappa\phi_m \int_{\Omega\times\mathbb{R}^d} \left|v^d - v_*^d\right|^2 f f_*\, dx dv\, dx_* dv_* \\
&= -2\kappa\phi_m \mathcal{E}_d.
\end{aligned}$$

Here, we used the mass and the d-coordinate momentum conservation laws for the last equality. Finally, we combine two estimates for $\mathcal{I}_{11}$ and $\mathcal{I}_{12}$ to obtain Grönwall's inequality for $\mathcal{E}_d$:

$$\frac{d\mathcal{E}_d}{dt} \le -2\kappa\phi_m \mathcal{E}_d.$$

This implies the desired estimate. ∎

5. Classical solutions to the kinetic model for $\Omega = [0,1] \times \mathbb{R}$. In this section, we present a global existence of classical solutions to the initial-boundary value problem (8). For simplicity, we consider the spatial domain $\Omega := [0,1] \times \mathbb{R}$ and we set the coupling strength κ to be 1 to avoid unnecessary complexity. A general case can be treated by the same argument. We will follow a similar technique developed in [20] for the Vlasov-Poisson system. More precisely, we use the standard successive approximation scheme to construct a classical solution for the velocity flux $F[f]$ and the specular reflection boundary condition, simultaneously.

5.1. Construction of approximate solutions. We now sketch the successive iterations as follows. For the zeroth order iteration f^0, we set

$$f^0(t,x,v) := f_0(x,v),$$

where the initial datum f_0 is a $\mathcal{C}^{1,\alpha}$-nonnegative normalized distribution:

$$f_0 \in C^{1,\alpha}(\Omega \times \mathbb{R}^2), \quad \int_{\Omega\times\mathbb{R}^2} f_0(x,v)\, dx dv = 1 \quad \text{and} \quad f_0 \ge 0.$$

Suppose that the n-th iterate f^n has already been constructed for $n \geq 0$. Then, the $(n+1)$-th iterate f^{n+1} is defined as a unique solution to the following linear system:

$$\begin{aligned} &\partial_t f^{n+1} + v \cdot \nabla_x f^{n+1} + \nabla_v \cdot \left(F\left[f^n\right] f^{n+1} \right) = 0, \quad (x,v) \in \Omega \times \mathbb{R}^2, \ t > 0, \\ &F^k[f^n](t,x,v) := \kappa \delta_{k2} \int_{\Omega \times \mathbb{R}^2} \phi(x - x_*)(v_*^k - v^k) f^n(t, x_*, v_*)\, dx_* dv_*, \quad k = 1, 2, \end{aligned} \tag{23}$$

subject to the initial and boundary conditions satisfying the compatibility conditions:

$$\begin{aligned} &f^{n+1}(0,x,v) = f_0(x,v), \quad (x,v) \in \Omega \times \mathbb{R}^2, \\ &f^{n+1}(t,0,x^2,v^1,v^2) = f^n(t,0,x^2,-v^1,v^2), \quad v_1 > 0, \\ &f^{n+1}(t,1,x^2,v^1,v^2) = f^n(t,1,x^2,-v^1,v^2), \quad v_1 < 0, \\ &f_0(0,x^2,v^1,v^2) = f_0(0,x^2,-v^1,v^2), \quad f_0(1,x^2,v^1,v^2) = f_0(1,x^2,-v^1,v^2), \\ &v^1 \partial_{x^1} f_0(x^1,x^2,v^1,v^2) + v^1 \partial_{x^1} f_0(x^1,x^2,-v^1,v^2) = 0, \quad x^1 \in \{0,1\}. \end{aligned} \tag{24}$$

Note that the second and third compatibility conditions come from

$$\partial_t f^{n+1}(0,x^1,x^2,v^1,v^2) = \partial_t f^n(0,x^1,x^2,-v^1,v^2), \quad x^1 \in \{0,1\}.$$

We rewrite the equation (23) as a quasilinear form:

$$\begin{aligned} &\partial_t f^{n+1} + v \cdot \nabla_x f^{n+1} + F[f^n] \cdot \nabla_v f^{n+1} \\ &\qquad = -\nabla_v \cdot F\left[f^n\right] f^{n+1} = \left[\int_{\Omega \times \mathbb{R}^2} \phi(x - x_*) f^n(t, x_*, v_*)\, dx_* dv_* \right] f^{n+1}. \end{aligned} \tag{25}$$

Next, we consider the characteristic curves $(x_{n+1}(s;t,x,v), v_{n+1}(s;t,x,v))$ for the equation (25) defined as

$$\begin{cases} \dfrac{dx_{n+1}}{ds} = v_{n+1}(s), \\ \dfrac{dv_{n+1}^k}{ds} = F^k\left[f^n\right](s, x_{n+1}(s), v_{n+1}(s)) \\ \qquad\qquad = \delta_{k2} \displaystyle\int_{\Omega \times \mathbb{R}^2} \phi(x_{n+1}(s) - x_*)(v_*^k - v_{n+1}^k(s)) f^n(s, x_*, v_*)\, dx_* dv_*, \\ x_{n+1}(t) = x, \quad v_{n+1}(t) = v. \end{cases} \tag{26}$$

Then, along this characteristic curves, we can explicitly write down the solution of (25). For this, we set a spatial-temporal domain Π and its boundaries. For a fixed time T,

$$\begin{aligned} &\Pi := [0,T] \times \Omega \times \mathbb{R}^2, \quad \Pi_0 := \left\{ (t,x,v) \in \Pi \mid x \in \Omega, \quad v \in \mathbb{R}^2, \quad t = 0 \right\}, \\ &\gamma_0 := \left\{ (t,x,v) \in \Pi \mid x^1 = 0, \ v^1 > 0, \ t > 0 \right\}, \\ &\gamma_1 := \left\{ (t,x,v) \in \Pi \mid x^1 = 1, \ v^1 < 0, \ t > 0 \right\}. \end{aligned}$$

Then, the characteristic curves $(x_{n+1}(s), v_{n+1}(s))$ which pass through the point $(t,x,v) \in \Pi$ can be classified into the following two cases:

1. The characteristic curve is from the initial layer, $(0, x_{n+1}(0), v_{n+1}(0)) \in \Pi_0$.
2. There exists $t_0 > 0$ such that $(t_0, x_{n+1}(t_0), v_{n+1}(t_0)) \in \gamma_0 \cup \gamma_1$.

For the case (1), we use the characteristic structure (25) to obtain

$$
\begin{aligned}
f^{n+1}(t,x,v) &= f_0(x_{n+1}(0), v_{n+1}(0)) \\
&\quad \times \exp\left[\int_0^t \int_{\Omega\times\mathbb{R}^2} \phi(x_{n+1}(s)-x_*) f^n(s,x_*,v_*)\, dx_* dv_*\, ds\right].
\end{aligned} \tag{27}
$$

For the case (2), we have

$$
\begin{aligned}
f^{n+1}(t,x,v) &= f^{n+1}(t_0, x_{n+1}(t_0), v_{n+1}(t_0)) \\
&\quad \times \exp\left[\int_{t_0}^t \int_{\Omega\times\mathbb{R}^2} \phi(x_{n+1}(s)-x_*) f^n(s,x_*,v_*)\, dx_* dv_*\, ds\right],
\end{aligned} \tag{28}
$$

where the boundary condition gives the value of f^{n+1} at t_0. In order to show that the solution defined by (27)–(28) is a classical solution to (23), we need to check that the two representations (27) and (28) coincide, when the characteristic curve is issued from the corner of Π_0:

$$
\big\{(t,x,v)\in\Pi \mid t_0 = 0,\ x^1_{n+1}(t_0)\in\{0,1\}\big\}.
$$

Before we deal with this, we state several technical lemmas.

LEMMA 5.1. *Suppose that $(t,x,v)\in\mathbb{R}_+\times\Omega\times\mathbb{R}^2$ is connected to $(0,x_0,v_0)$ through a characteristic curve defined by (26). Then, (x,v) and (x_0,v_0) satisfy the following relations:*

$$
\begin{aligned}
&v_0^1 = v^1, \quad v_0^2 = v^2 + \int_t^0 F^2[f^n](s, x_{n+1}(s), v_{n+1}(s))\, ds, \\
&x_0^1 = x^1 - v^1 t, \quad x_0^2 = x^2 - v^2 t + \int_t^0 \int_t^s F^2[f^n](\tau, x_{n+1}(\tau), v_{n+1}(\tau))\, d\tau\, ds.
\end{aligned} \tag{29}
$$

Moreover, if we interpret x_0 and v_0 as a function of t, x and v, then

$$
\begin{aligned}
\partial_{v^j} v_0^i &= \delta_{ij} + \delta_{i2} \int_t^0 \partial_{v^j} F^2[f^n](s, x_{n+1}(s), v_{n+1}(s))\, ds, \\
\partial_t v_0^i &= -\delta_{i2} F^2[f^n](t,x,v) + \delta_{i2} \int_t^0 \partial_t F^2[f^n](s, x_{n+1}(s), v_{n+1}(s))\, ds, \\
\partial_{x^j} v_0^i &= \delta_{i2} \int_t^0 \partial_{x^j} F^2[f^n](s, x_{n+1}(s), v_{n+1}(s))\, ds, \\
\partial_{v^j} x_0^i &= -\delta_{ij} t + \delta_{i2} \int_t^0 \int_t^s \partial_{v^j} F^2[f^n](\tau, x_{n+1}(\tau), v_{n+1}(\tau))\, d\tau\, ds, \\
\partial_t x_0^i &= -v^i + t\delta_{i2} F^2[f^n](t,x,v) + \delta_{i2} \int_t^0 \int_t^s \partial_t F^2[f^n](\tau, x_{n+1}(\tau), v_{n+1}(\tau))\, d\tau\, ds, \\
\partial_{x_j} x_0^i &= \delta_{ij} + \delta_{i2} \int_t^0 \int_t^s \partial_{x^j} F^2[f^n](\tau, x_{n+1}(\tau), v_{n+1}(\tau))\, d\tau\, ds.
\end{aligned}
$$

Proof. The relation (29) directly follows from the definition of characteristic curve (26), and the derivatives are from the relations (29). For example, for the formula of

$\partial_{v^j} v_0^i$, we differentiate the i-th component of (29) with respect to v^j to get

$$\begin{aligned}\partial_{v^j} v_0^i &= \partial_{v^j} v^i + \int_t^0 \partial_{v^j} F^i[f^n](s, x_{n+1}(s), v_{n+1}(s))\, ds \\ &= \delta_{ij} + \delta_{i2} \int_t^0 \partial_{v^j} F^2[f^n](s, x_{n+1}(s), v_{n+1}(s))\, ds.\end{aligned}$$

This yields the desired result. ∎

LEMMA 5.2. *Suppose that $(t, x, v) \in \mathbb{R}_+ \times \Omega \times \mathbb{R}^2$ is connected to (t_0, x_0, v_0), where $t_0 > 0$, $x_0^1 \in \{0, 1\}$ and $v_0^1 \neq 0$, through a characteristic curve defined in (26). Then, (x, v) and (x_0, v_0) satisfy the following relations:*

(30)
$$\begin{aligned}&v_0^1 = v^1, \quad v_0^2 = v^2 + \int_t^{t_0} F^2[f^n](s, x_{n+1}(s), v_{n+1}(s))\, ds, \quad x_0^1 = x^1 - v^1(t - t_0), \\ &x_0^2 = x^2 - v^2(t - t_0) + \int_t^{t_0} \int_t^s F^2[f^n](\tau, x_{n+1}(\tau), v_{n+1}(\tau))\, d\tau\, ds.\end{aligned}$$

Moreover, if we regard (t_0, x_0, v_0) as a function of (t, x, v), then we have

$$\begin{aligned}\partial_{v^j} t_0 &= \frac{\delta_{1j}(t - t_0)}{v_0^1}, \quad \partial_t t_0 = 1, \quad \partial_{x^j} t_0 = -\frac{\delta_{1j}}{v_0^1}, \\ \partial_{v^j} v_0^i &= \delta_{ij} + \frac{\delta_{i2}\delta_{1j}(t - t_0)}{v_0^1} F^2[f^n](t_0, x_{n+1}(t_0), v_{n+1}(t_0)) \\ &\quad + \delta_{i2} \int_t^{t_0} \partial_{v^j} F^2[f^n](s, x_{n+1}(s), v_{n+1}(s))\, ds, \\ \partial_t v_0^i &= \delta_{i2} F^2[f^n](t_0, x_{n+1}(t_0), v_{n+1}(t_0)) - \delta_{i2} F^2[f^n](t, x, v) \\ &\quad + \delta_{i2} \int_t^{t_0} \partial_t F^2[f^n](s, x_{n+1}(s), v_{n+1}(s))\, ds, \\ \partial_{x^j} v_0^i &= -\frac{\delta_{i2}\delta_{1j}}{v_0^1} F^2[f^n](t_0, x_{n+1}(t_0), v_{n+1}(t_0)) \\ &\quad + \delta_{i2} \int_t^{t_0} \partial_{x^j} F^2[f^n](s, x_{n+1}(s), v_{n+1}(s))\, ds, \\ \partial_{v^j} x_0^i &= -\delta_{ij}(t - t_0) + v_0^i \frac{\delta_{1j}(t - t_0)}{v_0^1} \\ &\quad + \delta_{i2} \int_t^{t_0} \int_t^s \partial_{v^j} F^2[f^n](\tau, x_{n+1}(\tau), v_{n+1}(\tau))\, d\tau\, ds, \\ \partial_t x_0^i &= -v^i + v_0^i + \delta_{i2}(t - t_0) F^2[f^n](t, x, v) \\ &\quad + \delta_{i2} \int_t^{t_0} \int_t^s \partial_t F^2[f^n](\tau, x_{n+1}(\tau), v_{n+1}(\tau))\, d\tau\, ds, \\ \partial_{x^j} x_0^i &= \delta_{ij} + v_0^i \partial_{x^j} t_0 + \delta_{i2} \int_t^{t_0} \int_t^s \partial_{x^j} F^2[f^n](\tau, x_{n+1}(\tau), v_{n+1}(\tau))\, d\tau\, ds.\end{aligned}$$

Proof. As in Lemma 5.1, the relation (30) directly follows from the definition of characteristic curve (26) and the derivatives are from the relation (30). Since the proof of derivatives are similar to that of Lemma 5.1, we only state the derivation of

the formula for $\partial_{v^j} t_0$. Since the characteristic curve collides with the boundary at t_0, we have

$$1 \text{ (or } 0) = x_0^1 = x^1 - v^1(t - t_0). \tag{31}$$

We take the v^j-derivative on (31) to obtain

$$0 = 0 - \delta_{1j}(t - t_0) + v^1(\partial_{v^j} t_0),$$

which is equivalent to

$$\partial_{v^j} t_0 = \frac{\delta_{1j}(t - t_0)}{v^1} = \frac{\delta_{1j}(t - t_0)}{v_0^1}.$$

Here, the last equality is due to $F^1[f^n] \equiv 0$. ∎

Under the boundary condition and compatibility conditions, two formulas (27) and (28) coincide when $(t_0, x_0^1, x_0^2, v_0^1, v_0^2) = (0, 0, x^2, v^1, v^2)$ or $(0, 1, x^2, v^1, v^2)$. In Proposition 5.3 in the next subsection, we check this coincidence for $t_0 \to 0$ on the set

$$\big\{(t, x, v) \in \Pi \mid t_0 = 0,\ x_{n+1}^1(t_0) \in \{0, 1\}\big\},$$

by using Lemma 5.1 and Lemma 5.2. Then, we can see that the function f^{n+1} lies in $\mathcal{C}^1(\mathrm{int}(\Pi))$, where $\mathrm{int}(\Pi)$ is the interior of Π.

5.2. Basic estimates on approximate solutions. In this subsection, we provide $\mathcal{C}^{1,\alpha}$-estimate of approximate solutions $\{f^n\}$.

PROPOSITION 5.3. *The solution of* (25) *given by formula* (27) *and* (28) *is contained in* $\mathcal{C}^1(\mathrm{int}(\Pi))$.

Proof. Note that we need to check that the two formulas (27) and (28) have the same values and the same first derivatives at (t, x, v), when its characteristic curve is issued from (t_0, x_0, v_0) for $t_0 = 0$ and $x_0^1 \in \{0, 1\}$. It is straightforward to see that the formulas (27) and (28) have the same value, as $t_0 \to 0$. Next, we need to check that two formulas have the same first derivatives when $t_0 \to 0$. We take the first-order time derivative on the formula (27) to obtain

$$\begin{aligned}
\partial_t f^{n+1}(t, x, v) = \Bigg[& \sum_{j=1}^{2} \partial_{x^j} f_0(x_0, v_0) \cdot \partial_t x_0^j + \sum_{j=1}^{2} \partial_{v^j} f_0(x_0, v_0) \cdot \partial_t v_0^j \\
& + f_0(x_0, v_0) \Bigg(\int_{\Omega \times \mathbb{R}^2} \phi(x - x_*) f^n(t, x_*, v_*)\, dx_* dv_* \\
& + \int_0^t \frac{d}{dt} \int_{\Omega \times \mathbb{R}^2} \phi(x_{n+1}(\tau) - x_*) f^n(\tau, x_*, v_*) dx_* dv_* d\tau \Bigg) \Bigg] \\
& \times \exp\left[\int_0^t \int_{\Omega \times \mathbb{R}^2} \phi(x_{n+1}(\tau) - x_*) f^n(\tau, x_*, v_*)\, dx_* dv_* d\tau \right].
\end{aligned} \tag{32}$$

On the other hand, we use (28) to get

$$
\begin{aligned}
\partial_t f^{n+1}(t,x,v) = \Bigg[& \partial_t f^{n+1}(t_0,x_0,v_0)\cdot\partial_t t_0 + \partial_{x^2} f^{n+1}(t_0,x_0,v_0)\cdot\partial_t x_0^2 \\
& + \sum_{j=1}^{2} \partial_{v^j} f^{n+1}(t_0,x_0,v_0)\cdot\partial_t v_0^j \\
& + f^{n+1}(t_0,x_0,v_0)\Bigg(\int_{\Omega\times\mathbb{R}^2} \phi(x-x_*) f^n(t,x_*,v_*)\,dx_*dv_* \\
& - \partial_t t_0 \cdot \int_{\Omega\times\mathbb{R}^2} \phi(x_0-x_*) f^n(t_0,x_*,v_*)\,dx_*dv_* \\
& + \int_{t_0}^{t} \frac{d}{dt} \int_{\Omega\times\mathbb{R}^2} \phi(x_{n+1}(\tau)-x_*) f^n(\tau,x_*,v_*)\,dx_*dv_*d\tau \Bigg)\Bigg] \\
& \times \exp\left[\int_{t_0}^{t} \int_{\Omega\times\mathbb{R}^2} \phi(x_{n+1}(\tau)-x_*) f^n(\tau,x_*,v_*)\,dx_*dv_*d\tau \right].
\end{aligned} \tag{33}
$$

We emphasize that t_0, x_0, v_0 in (32) and (33) are functions of (t,x,v). Since the first formula (32) is described by the initial datum f_0, we want to derive (32) from (33). We may use the results in Lemma 5.1 and Lemma 5.2, in particular,

$$
\partial_t t_0 = 1, \quad \partial_t v_0^1 = 0. \tag{34}
$$

On the other hand, we use the boundary condition:

$$
f^{n+1}(t,x,v^1,v^2) = f^n(t,x,-v^1,v^2), \quad x^1 \in \{0,1\},
$$

to get

$$
\begin{aligned}
\partial_t f^{n+1}(0,x,v^1,v^2) &= \partial_t f^n(0,x,-v^1,v^2) \\
&= \left(-v\cdot\nabla_x f^n - \partial_{v^2}(F^2[f^{n-1}]f^n)\right)\Big|_{(0,x,-v^1,v^2)},
\end{aligned}
$$

where $x^1 \in \{0,1\}$. Therefore, for x_0 such that $x_0^1 \in \{0,1\}$, we have

$$
\begin{aligned}
\partial_t f^{n+1}(t,x,v)\Big|_{(0,x_0,v_0)} &= \Bigg(- v^1\partial_{x^1} f^n - v^2\partial_{x^2} f^n - F^2[f^{n-1}]\partial_{v^2} f^n \\
&\quad + f^n \int_{\Omega\times\mathbb{R}^2} \phi(x-x_*) f^{n-1}(t,x_*,v_*)\,dx_*dv_* \Bigg)\Big|_{(0,x_0,-v_0^1,v_0^2)} \\
&= v_0^1\partial_{x^1} f_0(x_0,-v_0^1,v_0^2) - v_0^2\partial_{x^2} f_0(x_0,-v_0^1,v_0^2) - F^2[f_0]\partial_{v^2} f_0 \\
&\quad + f_0 \int_{\Omega\times\mathbb{R}^2} \phi(x_0-x_*) f_0(t,x_*,v_*)\,dx_*dv_* \\
&= -v_0^1\partial_{x^1} f_0(x_0,v_0^1,v_0^2) - v_0^2\partial_{x^2} f_0(x_0,v_0^1,v_0^2) - F^2[f_0]\partial_{v^2} f_0 \\
&\quad + f_0 \int_{\Omega\times\mathbb{R}^2} \phi(x_0-x_*) f_0(t,x_*,v_*)\,dx_*dv_* \\
&= \Big(- v\cdot\nabla_x f_0 - \partial_{v^2}\left(F^2[f_0]f_0\right)\Big)\Big|_{(x_0,v_0)}.
\end{aligned} \tag{35}
$$

Here, we used the boundary condition and compatibility condition (24) of the initial datum. We may apply the formulas (34) and (35), and Lemma 5.2 to the formula (33), then the right-hand side of (33) becomes

$$
\begin{aligned}
&\Bigg[- v_0^1 \partial_{x^1} f_0 - v_0^2 \partial_{x^2} f_0 - F^2[f_0](x_0,v_0)\partial_{v^2} f_0 + f_0 \int_{\Omega\times\mathbb{R}^2} \phi(x_0 - x_*) f_0(x_*,v_*)\, dx_* dv_* \\
&\quad + \partial_{x^2} f_0 \left(-v^2 + v_0^2 + tF^2[f^n](t,x,v) + \int_t^0 \int_t^s \partial_t F^2[f^n](\tau, x_{n+1}(\tau), v_{n+1}(\tau))\, d\tau\, ds \right) \\
&\quad + \partial_{v^2} f_0 \left(F^2[f_0](x_0,v_0) - F^2[f^n](x,v) + \int_t^0 \partial_t F^2[f^n](s, x_{n+1}(s), v_{n+1}(s))\, ds \right) \\
&\quad + f_0 \Bigg(\int_{\Omega\times\mathbb{R}^2} \phi(x - x_*) f^n(t,x_*,v_*)\, dx_* dv_* - \int_{\Omega\times\mathbb{R}^2} \phi(x_0 - x_*) f_0(x_*,v_*)\, dx_* dv_* \\
&\quad + \int_0^t \frac{d}{dt} \int_{\Omega\times\mathbb{R}^2} \phi(x_{n+1}(\tau) - x_*) f^n(\tau,x_*,v_*)\, dx_* dv_* d\tau \Bigg) \Bigg] \\
&\quad \times \exp\left[\int_0^t \int_{\Omega\times\mathbb{R}^2} \phi(x_{n+1}(\tau) - x_*) f^n(\tau,x_*,v_*)\, dx_* dv_* d\tau \right] \\
&= \Bigg[- v^1 \partial_{x^1} f_0 - v^2 \partial_{x^2} f_0 - F^2[f^n](x,v)\partial_{v^2} f_0 \\
&\qquad + \partial_{x^2} f_0 \left(tF^2[f^n](t,x,v) + \int_t^0 \int_t^s \partial_t F^2[f^n](\tau, x_{n+1}(\tau), v_{n+1}(\tau))\, d\tau\, ds \right) \\
&\qquad + \partial_{v^2} f_0 \left(\int_t^0 \partial_t F^2[f^n](s, x_{n+1}(s), v_{n+1}(s))\, ds \right) \\
&\qquad + f_0 \Bigg(\int_{\Omega\times\mathbb{R}^2} \phi(x - x_*) f^n(t,x_*,v_*)\, dx_* dv_* \\
&\qquad + \int_0^t \frac{d}{dt} \int_{\Omega\times\mathbb{R}^2} \phi(x_{n+1}(\tau) - x_*) f^n(\tau,x_*,v_*)\, dx_* dv_* d\tau \Bigg) \Bigg] \\
&\quad \times \exp\left[\int_0^t \int_{\Omega\times\mathbb{R}^2} \phi(x_{n+1}(\tau) - x_*) f^n(\tau,x_*,v_*)\, dx_* dv_* d\tau \right],
\end{aligned}
$$

where we abbreviate $f_0(x_0,v_0)$ as f_0 for simple notation. This equation is exactly the same as (32) combined with Lemma 5.1. We may show that the other derivatives are also the same in a similar manner. This implies that the constructed solution f^{n+1} is contained in $\mathcal{C}^1(\mathrm{int}(\Pi))$. ∎

REMARK 5.4. *Below, we discuss several comments on the results of Proposition 5.3.*

1. *From Proposition 5.3, the solution f is actually in $\mathcal{C}^1(\Pi \setminus \gamma^0)$,*

$$\text{where} \quad \gamma^0 := \left\{ (t,x,v) \mid x^1 = 0 \text{ or } 1 \quad \text{and} \quad v^1 = 0 \right\}.$$

The continuously differentiability including γ^0 needs more careful calculations, since t_0 is not well defined for γ^0.

2. *If the initial datum f_0 has a compact support detached from γ^0 in the sense that*

$$\operatorname{dist}\left(\operatorname{supp} f_0, \gamma^0 \cap \{t=0\}\right) > 0,$$

then, it follows from the characteristic formula (26) that the support of f^{n+1} is also detached from γ^0. More precisely, suppose that the support of f_0 does not contain $[0,r]\times\mathbb{R}\times[-r,r]\times\mathbb{R}$ for some $r>0$. Then, this set contains $\{(x,v)\mid x^1=0,\ v^1=0\}$ in its interior, which is a part of $\gamma_0\cap\{t=0\}$. The characteristics $x_{n+1}(s;t,x,v)$ and $v_{n+1}(s;t,x,v)$ with

$$(t,x,v)\in\{(t,x,v)\in\Pi\mid x^1\in[0,r],\ v^1\in[-r,r]\ \text{ and }\ x^1+|v^1|t<r\}$$

are from the initial layer, $(0,x_{n+1}(0),v_{n+1}(0))$, where $(x_{n+1}(0),v_{n+1}(0))\in[0,r]\times\mathbb{R}\times[-r,r]\times\mathbb{R}$. This implies that $\operatorname{supp} f^{n+1}$ is detached from the set $\{(t,x,v)\in\Pi\mid x^1=0,\ v^1=0\}$. The same property holds for $[1-r,1]\times\mathbb{R}\times[-r,r]\times\mathbb{R}$, so that the support of f^{n+1} remains detached from γ^0. Therefore, the $\mathcal{C}^1$-solution constructed above can be extended to the whole domain Π.

3. *The obtained $\mathcal{C}^1$-solution f^n has a uniformly bounded support if f_0 has a compact support. To show this, we recall the second equation of characteristic equation (26):*

$$\frac{dv^k_{n+1}}{ds}=\delta_{k2}\int_{\Omega\times\mathbb{R}^2}\phi(x_{n+1}(s)-x_*)\left(v^k_*-v^k_{n+1}(s)\right)f^n(x_*,v_*,s)\,dx_*\,dv_*.$$

It is clear that we only need to consider the d-th component, since the other components have compact spatial domain with bounded velocities. Let

$$D^2_{v0}:=\sup_{0\le t\le T}D^2_v\left(f^0(t)\right)=D^2_v\left(f_0\right)<\infty,$$

(see (19) for definition of $D^2_v(\cdot)$) and suppose that for induction on n, we have

$$\sup_{0\le t\le T}D^2_v(f^n(t))\le D^2_{v0}.$$

Consider the second coordinate of characteristic curve $(x^2_{n+1}(s),v^2_{n+1}(s))$ of the position and velocity. Then, it follows from the characteristic equation (26) that

$$\frac{dv^2_{n+1}}{ds}\le\left(\sup_{0\le t\le T}v^2_n\right)-v^2_{n+1},$$

$$\text{i.e.,}\ \ v^2_{n+1}(t)\le v^2_{n+1}(t_0)e^{-(t-t_0)}+\left(\sup_{0\le t\le T}v^2_n\right)\left(1-e^{-(t-t_0)}\right),$$

where $t_0=0$ or $x^1_{n+1}(t_0)\in\{0,1\}$. From the f^n-assumption,

$$v^2_{n+1}(t_0)\le D^2_{v0}\ \ \text{and}\ \ \sup_{0\le t\le T}v^2_n\le D^2_{v0},\quad \text{so that}\ \ v^2_{n+1}(t)\le D^2_{v0}.$$

From the mathematical induction on n, we have a bounded velocity support for any n:

$$v^2_n(t)\le D^2_{v0}.$$

It also holds for the infimum d-component velocity, $\inf v_n^2$*. Therefore, we have*

$$\sup_{0\le t\le T} D_v^2\left(f^n(t)\right) \le \sup_{0\le t\le T} D_v^2\left(f^0(t)\right), \quad n=0,1,2,\cdots.$$

The uniform boundedness of the d-th component of spatial support directly comes from the uniform boundedness of the velocity support.

5.3. Convergence of approximate solutions. In this subsection, we will show that the sequence of approximate solutions $\{f^n\}$ converge, and their limit is in fact a classical solution to (8). Next, we will show that the sequence of approximated solutions $\{f^n\}$ is uniformly bounded in the $\mathcal{C}^1$-space. Before we proceed further, we introduce notation for the several norms: For any fixed $T>0$, we set

$$|f(t)|_0 := \sup_{(x,v)\in\Omega\times\mathbb{R}^2} |f(t,x,v)|, \quad |f(t)|_1 := |\partial_t f(t)|_0 + |\nabla_x f(t)|_0 + |\nabla_v f(t)|_0,$$

$$\|f\|_0 := \sup_{0\le t\le T} |f(t)|_0, \quad \|f\|_1 := \sup_{0\le t\le T} |f(t)|_1.$$

PROPOSITION 5.5. *Let* $\{f^n\}$ *be a sequence of approximated solutions constructed by* (23) *for* $t\in[0,T]$*. Then, there exists a positive constant* C_T^0 *depending only* T *and* f_0*, such that*

$$\|f^n\|_0 + \|f^n\|_1 < C_T^0, \quad n=1,2,\cdots.$$

Proof. The proof relies on several ingredients, say, boundedness of velocities in Remark 5.4, characteristic formulas (27) and (28), and the induction arguments on n.

• Step A (Boundedness of the zeroth order): We use equations (27) and (28) to obtain boundedness of $\|f^n\|_0$.

⋄ (Case A.1): Suppose that the solution f^n is given by the formula (27). Then, it is straightforward to see

$$\begin{aligned}|f^{n+1}(t,x,v)| &\le |f_0|_0 \exp\left[\int_0^t \int_{\Omega\times\mathbb{R}^2} \phi(x_{n+1}(\tau)-x_*) f^n(\tau,x_*,v_*)\,dx_*dv_*\,d\tau\right]\\ &\le |f_0|_0 e^T,\end{aligned}$$

where we used $\phi\le 1$ and conservation of mass so that for all $\tau\ge 0$, we have

$$\int_{\Omega\times\mathbb{R}^2} \phi(x_{n+1}(\tau)-x_*) f^n(\tau,x_*,v_*)\,dx_*dv_* \le \int_{\Omega\times\mathbb{R}^2} f^n(\tau,x_*,v_*)\,dx_*dv_* = 1.$$

⋄ (Case A.2): Suppose that the solution f^n is given by the formula (28). Then, we use Case A.1 to see

$$\begin{aligned}|f^{n+1}(t,x,v)| &\le |f^{n+1}(t_0,x_{n+1}(t_0),v_{n+1}(t_0))|\\ &\quad\times \exp\left[\int_{t_0}^t \int_{\Omega\times\mathbb{R}^2} \phi(x_{n+1}(\tau)-x_*) f^n(\tau,x_*,v_*)\,dx_*dv_*\,d\tau\right]\\ &\le |f^{n+1}(t_0)|_0 e^{t-t_0}.\end{aligned}$$

This implies

$$|f^{n+1}(t)|_0 \le |f^{n+1}(t_0)|_0 e^{t-t_0}.$$

Note that we have the boundary condition:

$$f^{n+1}(t_0, x_0, v_0) = f^n(t_0, x_0, -v_0^1, v_0^2).$$

Hence, we can further proceed the estimation using the characteristics of f^n. Let (t_1, x_1, v_1) be the boundary value of the characteristic trajectory, which satisfy $t_1 = 0$ or $x_0^1 \in \{0, 1\}$ and $t_1 < t_0$. Then, we have the estimation on $|f^n(t_0)|_0$:

$$|f^n(t_0)|_0 \le |f^n(t_1)|_0 e^{t_0 - t_1}, \quad \text{so that} \quad |f^{n+1}(t)|_0 \le |f^n(t_1)|_0 e^{t-t_1}.$$

In this way, we can inductively estimate $|f^{n+1}(t)|_0$ until $t_l = 0$ for some $l < n$, or $t_l > 0$ with $l = n$, since n is finite. If $t_l = 0$, then we have

$$|f^{n+1}(t)|_0 \le |f_0|_0 e^t,$$

or if $t_n > 0$, then we have

$$|f^{n+1}(t)|_0 \le |f^0(t_n)|_0 e^{t-t_n} \le |f_0|_0 e^t.$$

Therefore, in any case, we have a uniform boundedness for $\|f^n\|_0$:

$$\|f^n\|_0 \le |f_0|_0 e^T. \tag{36}$$

• Step B (Boundedness of the first order): We also consider two cases. From Remark 5.4, we set

$$D_{v0}^2 = \sup_{0\le t\le T} D_v^2\left(f^0(t)\right), \quad \text{so that} \quad \sup_{0\le t\le T} D_v^2\left(f^n(t)\right) \le D_{v0}^2.$$

◇ (Case B.1): Suppose that the characteristics (x_{n+1}, v_{n+1}) given by (26) directly connect (t, x, v) to $\left\{(0, x, v) \ : \ x \in \Omega, \ v \in \mathbb{R}^2\right\}$. We take ∂_{x^i} to (25) to get the following estimate along the characteristic curve:

(37)

$$\begin{aligned}
&\frac{d}{ds}\partial_{x^i} f^{n+1} \\
&\quad = \left[\partial_t + v\cdot\nabla_x + F[f^n]\cdot\nabla_v\right](\partial_{x^i} f^{n+1}) \\
&\quad = -\partial_{x^i}(F[f^n])\cdot\nabla_v f^{n+1} - \partial_{x^i}\nabla_v\cdot F[f^n] f^{n+1} - \nabla_v\cdot F[f^n]\partial_{x^i} f^{n+1} \\
&\quad = -\partial_{x^i}(F[f^n])\cdot\nabla_v f^{n+1} + \partial_{x^i}\left[\int_{\Omega\times\mathbb{R}^2}\phi(x-x_*) f^n(s, x_*, v_*)\, dx_* dv_*\right] f^{n+1} \\
&\qquad + \left[\int_{\Omega\times\mathbb{R}^2}\phi(x-x_*) f^n(s, x_*, v_*)\, dx_* dv_*\right]\partial_{x^i} f^{n+1} \\
&\quad \le D_{v0}^2\|\nabla\phi\|_{L^\infty}|\nabla_v f^{n+1}(s)|_0 + \|\nabla\phi\|_{L^\infty}|f^{n+1}(s)|_0 + |\partial_{x^i} f^{n+1}(s)|_0 \\
&\quad \le D_{v0}^2\|\nabla\phi\|_{L^\infty}\sup_{0\le\tau\le t}|\nabla_v f^{n+1}(\tau)|_0 + \|\nabla\phi\|_{L^\infty}\sup_{0\le\tau\le t}|f^{n+1}(\tau)|_0 + |\partial_{x^i} f^{n+1}(s)|_0,
\end{aligned}$$

where we used the uniform boundedness of a velocity support. Here, $\|\cdot\|_{L^\infty}$ denotes usual L^∞-norm of function. Then, we apply Grönwall's lemma to (37) to get

$$\begin{aligned}|\nabla_x f^{n+1}(t,x,v)| \le |\nabla_x f_0|_0 e^t + D_{v0}^2\|\nabla\phi\|_{L^\infty}\sup_{0\le\tau\le t}|\nabla_v f^{n+1}(\tau)|_0(e^t-1)\\ + \|\nabla\phi\|_{L^\infty}\sup_{0\le\tau\le t}|f^{n+1}(\tau)|_0(e^t-1).\end{aligned}$$

Similarly, we can estimate the velocity derivatives of f^{n+1} as

$$\begin{aligned}&\frac{d}{ds}\partial_{v^i} f^{n+1}(t,x,v)\\ &\quad= -\partial_{v^i}(F[f^n])\cdot\nabla_v f^{n+1} - \partial_{v^i}\nabla_v\cdot F[f^n] f^{n+1} - \nabla_v\cdot F[f^n]\partial_{v^i} f^{n+1}\\ &\quad\le \delta_{i2}|\partial_{v^2} f^{n+1}|_0 + 0 + |\partial_{v^i} f^{n+1}|_0 \le 2|\partial_{v^i} f^{n+1}|_0,\end{aligned}$$

and hence

$$|\nabla_v f^{n+1}(t,x,v)| \le |\nabla_v f_0|_0 e^{2t}. \tag{38}$$

Then, we can close the estimate of spatial derivatives:

$$\begin{aligned}|\nabla_x f^{n+1}(t,x,v)| &\le |\nabla_x f_0|_0 e^t + \left(D_{v0}^2\|\nabla\phi\|_{L^\infty}|\nabla_v f_0|_0 e^{2t} + \|\nabla\phi\|_{L^\infty}|f_0|_0 e^t\right)(e^t-1)\\ &\le |\nabla_x f_0|_0 e^t + D_{v0}^2\|\nabla\phi\|_{L^\infty}|\nabla_v f_0|_0 e^{3t} + \|\nabla\phi\|_{L^\infty}|f_0|_0 e^{2t},\end{aligned} \tag{39}$$

where we used the estimate $|f^{n+1}(t)|_0 \le |f_0|_0 e^t$ from Step A. For the time derivatives, we may use the dynamics itself:

$$\begin{aligned}|\partial_t f^{n+1}(t,x,v)| &= \left|v\cdot\nabla_x f^{n+1} + \nabla_v\cdot(F[f^n]f^{n+1})\right|\\ &\le D_{v0}^2|\nabla_x f^{n+1}|_0 + |f^{n+1}|_0 + D_{v0}^2|\nabla_v f^{n+1}|_0.\end{aligned} \tag{40}$$

Now, we combine estimates (38)–(40), together with the zeroth-order estimate (36) to yield

$$\begin{aligned}&|f^{n+1}(t)|_0 + |f^{n+1}(t)|_1 \le (D_{v0}^2+1)(|\nabla_x f^{n+1}| + |\nabla_v f^{n+1}|) + 2|f^{n+1}|_0\\ &\quad\le \left((D_{v0}^2+1)D_{v0}^2\|\nabla\phi\|_{L^\infty} + (D_{v0}^2+1)\|\nabla\phi\|_{L^\infty} + (D_{v0}^2+1) + 2\right)e^{3t}(|f_0|_0 + |f_0|_1).\end{aligned}$$

This implies a uniform boundedness of $\|f^{n+1}\|_0 + \|f^{n+1}\|_1$.

$\diamond$ (Case B.2): Suppose that the characteristic $(x_{n+1}(s), v_{n+1}(s))$ given by (26) directly connects (t,x,v) to (t_0,x_0,v_0), which is $\gamma_0\cup\gamma_1$, that is, $t_0>0$. So we can estimate the velocity derivatives from the value of $f^{n+1}(t_0)$:

$$|\nabla_v f^{n+1}(t,x,v)| \le |\nabla_v f^{n+1}(t_0,x_0,v_0)|e^{2(t-t_0)}.$$

From t_0 to 0, we use the same arguments as in Step A. We may use the boundary condition to get

$$|\nabla_v f^{n+1}(t,x,v)| \le |\nabla_v f^{n}(t_0,x_0,-v_0^1,v_0^2)|e^{2(t-t_0)}.$$

Next, we can consider the characteristics $(x_n(s), v_n(s))$ connecting (t_0,x_0,v_0) with (t_1,x_1,v_1) to get

$$|\nabla_v f^{n+1}(t,x,v)| \le |\nabla_v f^{n}(t_0,x_0,-v_0^1,v_0^2)|e^{2(t-t_0)} \le |\nabla_v f^{n}(t_1,x_1,v_1)|e^{2(t-t_1)}.$$

Then, the induction argument on n leads us to the same estimates as in Case A:

$$|\nabla_v f^{n+1}(t,x,v)| \le |\nabla_v f_0|_0 e^{2t}.$$

Since the time derivative $|\partial_t f^{n+1}|_0$ directly depends on the other derivatives from (40), we only need to show that the estimates are also the same as the spatial derivatives. We can estimate $\partial_{x^i} f^{n+1}(s)$ for $t_0 \le s \le t$ using (37) as follows:

$$\frac{d}{ds}\partial_{x^i} f^{n+1} \le D_{v0}^2 \|\nabla\phi\|_{L^\infty} |\nabla_v f^{n+1}(s)|_0 + \|\nabla\phi\|_{L^\infty} |f^{n+1}(s)|_0 + |\partial_{x^i} f^{n+1}(s)|_0,$$

for the characteristic curve from (t,x,v) to (t_0,x_0,v_0). Considering the boundary condition, we need to estimate $\partial_{x^i} f^n$ at $(t_0,x_0,-v_0^1,v_0^2)$. However, we can estimate it similar to $\partial_{x^i} f^{n+1}$ as

$$\frac{d}{ds}\partial_{x^i} f^{n} \le D_{v0}^2 \|\nabla\phi\|_{L^\infty} |\nabla_v f^{n}(s)|_0 + \|\nabla\phi\|_{L^\infty} |f^{n}(s)|_0 + |\partial_{x^i} f^{n}(s)|_0, \quad t_1 \le s \le t_0,$$

for the characteristic curve from $(t_0,x_0,-v_0^1,v_0^2)$ to (t_1,x_1,v_1), and so on. Therefore, induction on n gives us the following rough estimate as in Case B.1:

$$\frac{d}{dt}\partial_{x^i} f^{n+1} \le D_{v0}^2 \|\nabla\phi\|_{L^\infty} |\nabla_v f_0|_0 e^{2t} + \|\nabla\phi\|_{L^\infty} |f_0|_0 e^{t} + |\partial_{x^i} f^{n+1}(t)|_0.$$

This yields

$$|\nabla_x f^{n+1}(t,x,v)| \le |\nabla_x f_0|_0 e^{t} + D_{v0}^2 \|\nabla\phi\|_{L^\infty} |\nabla_v f_0|_0 e^{3t} + \|\nabla\phi\|_{L^\infty} |f_0|_0 e^{2t}.$$

Therefore, with the time derivative (40), we have the same estimate as in Case B.1:

$$\begin{aligned} &|f^{n+1}(t)|_0 + |f^{n+1}(t)|_1 \le (D_{v0}^2+1)(|\nabla_x f^{n+1}| + |\nabla_v f^{n+1}|) + 2|f^{n+1}|_0 \\ &\le \left((D_{v0}^2+1)D_{v0}^2\|\nabla\phi\|_{L^\infty} + (D_{v0}^2+1)\|\nabla\phi\|_{L^\infty} + (D_{v0}^2+1) + 2\right) e^{3t}(|f_0|_0 + |f_0|_1). \end{aligned}$$

This implies a uniform boundedness of $\|f^{n+1}\|_0 + \|f^{n+1}\|_1$. ∎

With the $\mathcal{C}^1$-boundedness of $\{f^n\}_{n\ge 0}$ and $\mathcal{C}^{1,\alpha}$-regularity on the initial datum and communication weight, we are able to obtain the following uniform $\mathcal{C}^{1,\alpha}$-estimate as in [20].

PROPOSITION 5.6. *Suppose that the initial datum and communication weight are nonnegative Hölder continuous in the sense that*

$$0 \le f_0 \in C^{1,\alpha}(\Omega \times \mathbb{R}^2), \quad 0 \le \phi \in C^{1,\alpha}(\Omega),$$

and let $\{f^n\}$ be a sequence of approximated solutions constructed by (23) for $t \in [0,T]$. Then, there exists a positive constant C_T^0 depending only T and f_0, such that

$$\|f^n\|_{C^{1,\alpha}(\mathrm{int}(\Pi))} < C_T^0, \quad n = 1,2,\dots.$$

Proof. Since we have already obtained a uniform $\mathcal{C}^1$-boundedness of f^n in Proposition 5.5 and the number of collision with boundary is finite, we can repeat exactly the same argument in [20, Section 4] to obtain a uniform boundedness in Hölder norm as well. Thus, we omit its details. ∎

We are now ready to present a global existence of the solution to the kinetic C-S model (8).

THEOREM 5.7. *Suppose that the initial datum f_0 and communication weight ϕ satisfy the following conditions:*

1. *f_0 is $\mathcal{C}^{1,\alpha}$-regular, nonnegative normalized and compactly supported.*
2. *f_0 satisfies the compatibility condition (24).*
3. *ϕ is $\mathcal{C}^{1,\alpha}$-regular and satisfies (2).*

Then, for $0 < \beta < \alpha$, there exist the unique solution $f \in C^{1,\beta}(\mathrm{int}(\Pi))$ to the kinetic Cucker-Smale model (8).

Proof. • (Existence part): Note that Proposition 5.6 implies that $\{f^n\}_{n\geq 0}$ is bounded in the space $\mathcal{C}^{1,\alpha}$. Moreover, Remark 5.4 implies that the sequence of approximate solutions $\{f^n\}_{n\geq 0}$ has uniformly bounded compact support. Therefore, by Arzela-Ascoli theorem, there exist a subsequence, still denoted as $\{f^n\}$, such that

$$f^n \to f \text{ in } \mathcal{C}^{1,\beta}(\mathrm{int}(\Pi)), \quad \text{for} \quad 0 < \beta < \alpha.$$

• (Uniqueness part): Let f_1 and f_2 be two classical solutions of the kinetic C-S model with the same initial data. We set $\delta f := f_1 - f_2$. Then, the difference δf satisfies the following inequality: for $t \in [0, T]$,

$$\begin{aligned}
\frac{d}{dt}\delta f &= \frac{d}{dt}f_1 - \frac{d}{dt}f_2 \\
&= [\partial_t + v\cdot\nabla_x + F[f_1]\cdot\nabla_v]f_1 - [\partial_t + v\cdot\nabla_x + F[f_2]\cdot\nabla_v]f_2 \\
&= -\nabla_v\cdot F[f_1]f_1 + \nabla_v\cdot F[f_2]f_2 \\
&= \partial_{v^2}F^2[f_2]f_2 - \partial_{v^2}F^2[f_1]f_1 \\
&= -\int_{\Omega\times\mathbb{R}^2}\phi(x-x_*)f_2(t,x,v)f_2(t,x_*,v_*)\,dx_*dv_* \\
&\quad + \int_{\Omega\times\mathbb{R}^2}\phi(x-x_*)f_1(t,x,v)f_1(t,x_*,v_*)\,dx_*dv_* \\
&= -\int_{\Omega\times\mathbb{R}^2}\phi(x-x_*)(f_2(t,x,v)-f_1(t,x,v))f_2(t,x_*,v_*)\,dx_*dv_* \\
&\quad - \int_{\Omega\times\mathbb{R}^2}\phi(x-x_*)f_1(t,x,v)(f_2(t,x_*,v_*)-f_1(t,x_*,v_*))\,dx_*dv_*.
\end{aligned}$$

Therefore, we multiply $\mathrm{sgn}(\delta f)$ and take a supremum over Π to get an inequality of $|\delta f|_0$:

$$\begin{aligned}
\frac{d}{dt}|\delta f|_0 &\leq |f_1 - f_2|_0 \int_{\Omega\times\mathbb{R}^2} f_2(t,x_*,v_*)\,dx_*\,dv_* \\
&\quad + |f_1|_0 \int_{\Omega\times\mathbb{R}^2} |f_2(t,x_*,v_*) - f_1(t,x_*,v_*)|\,dx_*\,dv_* \\
&\leq |f_1 - f_2|_0 + CC_T^0|f_1 - f_2|_0 = (1 + CC_T^0)|\delta f|_0,
\end{aligned} \tag{41}$$

for the constant C_T^0 as in Proposition 5.2 by taking the limit $n \to \infty$ and some constant C depending on the bounded supports of $f_1(t)$ and $f_2(t)$. Next, we apply Grönwall's lemma to (41) and conclude that

$$|\delta f(t)|_0 \leq \tilde{C}_t|\delta f(0)|_0,$$

for some constant $\tilde{C}_t$. Since $f_1(0) = f_2(0)$, $|\delta f(0)|_0 = 0$ and hence $|\delta f(t)|_0$=0. This implies the uniqueness of solution to the kinetic C-S model. ∎

6. Numerical Simulations. In this section, we present several numerical results for the particle and kinetic Cucker-Smale models with the specular reflection boundary condition. We conduct numerical simulations for both the original flocking model (1) with (4) and the flow-directional flocking model (7). We also perform simulations for two corresponding kinetic C-S models as well, and then compare them with theoretical results obtained in Section 3.

6.1. The particle model. First, we perform numerical simulations for the two-dimensional Cucker-Smale particle model. For numerical simulations, we used the fourth-order Runge-Kutta method and choose the spatial dimension, coupling strength and communication weight as follows:

$$d = 2, \quad \kappa = 2, \quad \phi(x) = \frac{1}{1+|x|}.$$

We use 200 random particles of which initial positions are uniformly distributed on $[0,1] \times [0,1]$ and initial velocities are also uniformly distributed on $[0,2] \times [0,2]$. We assume the specular reflection boundary condition on $x^1 = 0$ and $x^1 = 1$, and the periodic boundary condition on $x^2 = 0$ and $x^2 = 1$. Hence, the spatial domain is the periodic channel. Fig. 2(a) shows one of the realizations of the initial data.

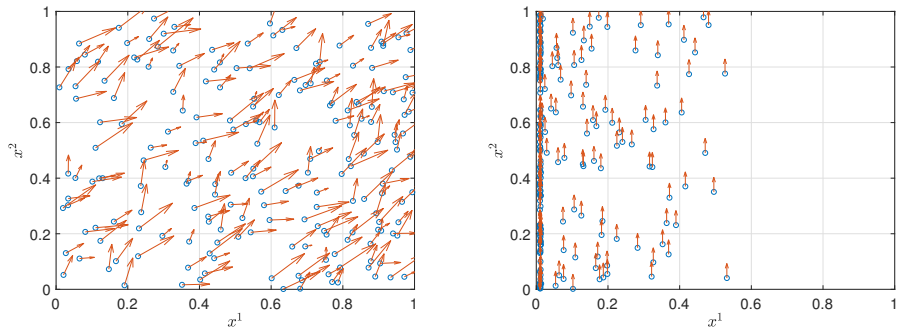

(a) Initial data (b) Position and velocities at $t = 10$

FIG. 2. *Numerical result for the original C-S model. Periodic boundary condition is employed on* $x^2 = 0$ *and* $x^2 = 1$

Fig. 2(b) shows the result for the original flocking model, (1) with (4). Similar to the two-particle system in Section 2, we observe that many particles stick to the boundary and lose the uniform distribution. Fig. 3 shows the result for the flow-directional flocking force under the same initial data. Since there is no force along the x^1-axis, each particle maintains their own initial x^1-directional velocity. In Fig. 3(a), the velocities of particles seems not to be aligned at all. However, when we plot velocities only along the v^2-axis, in Fig. 3(b), the x^2-directional velocities are already well aligned.

Fig. 4 shows the numerical values and theoretical upper bounds of the flocking rate on the x^2-directional velocities. In Theorem 3.2, we have the flow-directional flocking estimate:

$$D_v^2(t) \le D_v^2(0) e^{-\kappa\tilde{\phi}\left(x_d^\infty + D(\tilde{\Omega})\right)t}.$$

In our numerical example, the whole spatial domain Ω is bounded and we may take the smallest value of $\tilde{\phi}$ instead of $\tilde{\phi}\left(x_d^\infty + D(\tilde{\Omega})\right)$. Therefore, in this case, the theoretical

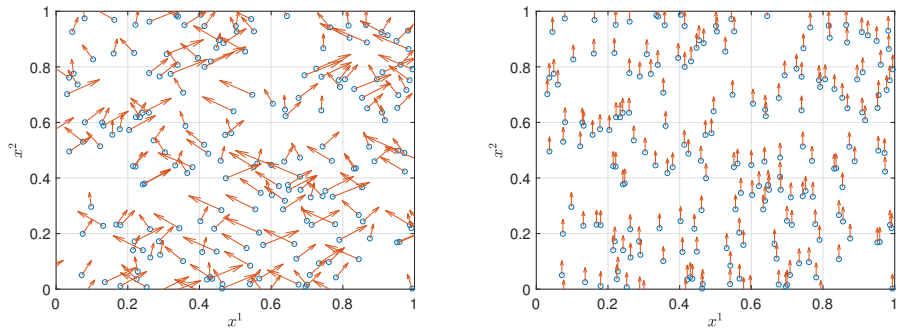

(a) The whole velocity vectors (b) The x^2-directional velocities

FIG. 3. *Numerical result for the C-S model with the flow-directional flocking force at* $t = 10$

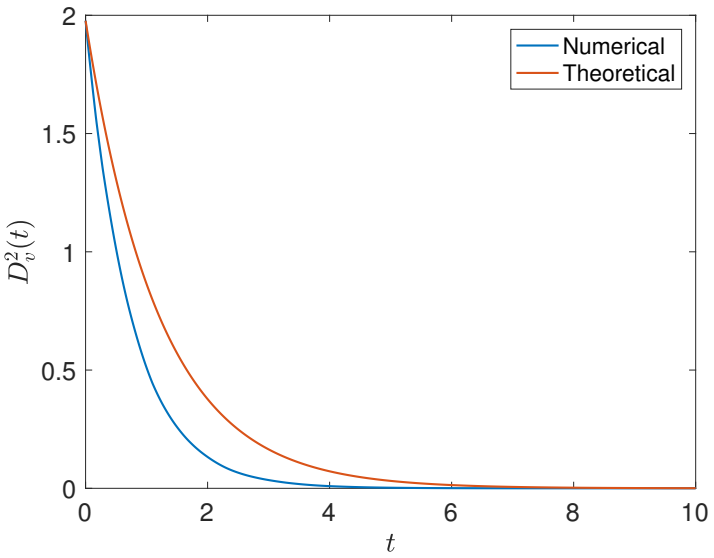

FIG. 4. *A flocking estimate for* x^2*-directional velocities*

decay rate is at least $D_v^2(0)e^{-2\tilde{\phi}(\sqrt{2})t}$, which is drawn by the red curve in Fig. 4. The blue curve in Fig. 4 shows a numerical decay rate of diameter of x^2-directional velocities, which is plotted from the result in Fig. 3. The numerical data decays faster than the theoretical one, so it validates the result of Theorem 3.2.

Finally, we present the numerical simulation for the three-dimensional C-S model in the periodic cylinder $\overline{B_1(0)} \times [0,1]$. We chose the 200 random initial particles, whose positions are uniformly distributed on $\overline{B_1(0)} \times [0,1]$ and initial velocities are uniformly distributed on $[-1,1] \times [0,2] \times [0,1]$. Fig. 5(a) is one of the realization of the initial data. As the mean value of initial velocity along x^1 and x^2 direction are 0 and 1 respectively, we can expect that the ensemble of the original C-S flocking model will aggregate on the boundary near $(x^1, x^2) = (0,1)$. This expected phenomenon is observed in numerical simulation, which is illustrated in Fig. 5(b)–Fig. 5(d), in

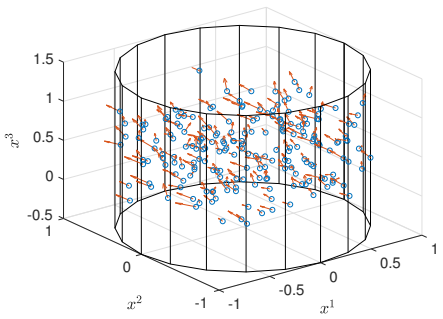

(a) Initial data

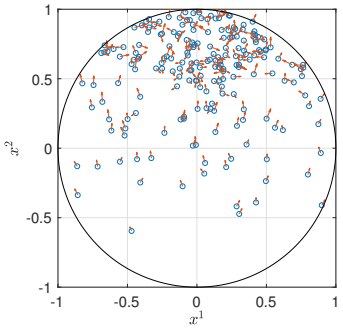

(b) Particle ensemble projected onto (x^1, x^2)-space at $t = 1$

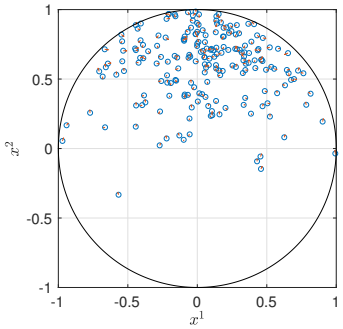

(c) Particle ensemble projected onto (x^1, x^2)-space at $t = 2$

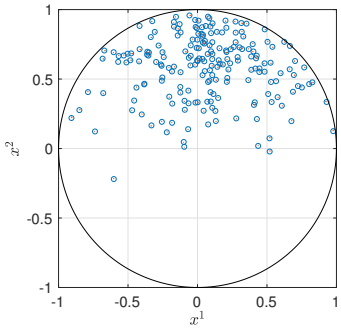

(d) Particle ensemble projected onto (x^1, x^2)-space at $t = 3$

FIG. 5. *Numerical result for the original three-dimensional C-S model*

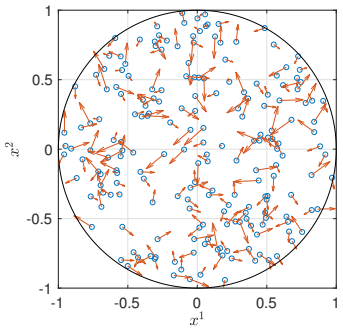

(a) Particle ensemble and (v^1, v^2)-velocity vectors projected onto (x^1, x^2)-space at $t = 3$

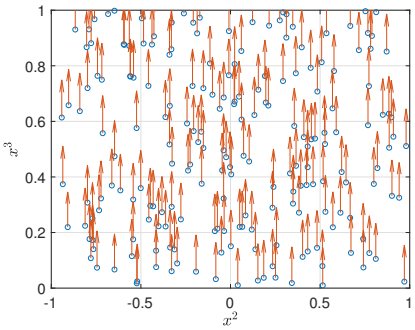

(b) The v^3-directional velocities projected onto (x^2, x^3)-space

FIG. 6. *Numerical result for the three-dimensional C-S model with the flow-directional flocking force at $t = 3$. Periodic boundary condition is employed on $x^3 = 0$ and $x^3 = 1$*

which the projection of particle ensemble onto (x^1, x^2)-space is presented. In the case of flow-directional flocking model, we observe in Fig. 6 that a similar behavior as in the

2-dimensional case emerges. Again, in Fig. 6(a), the velocities along (v^1, v^2)-direction is not aligned. We provide the projected particle ensemble onto (x^2, x^3)-space in Fig. 6(b). We can observe that the v^3-direction of velocities are aligned.

6.2. The kinetic model. We next conduct the numerical simulations for the kinetic C-S model with the specular reflection boundary condition. For numerical simulations, we used the third-order ENO method with upwind directions and the third-order TVD Runge-Kutta method. As in the C-S model, we set the spatial domain as a periodic channel $\Omega := [-1, 1] \times \mathbb{T}$, $\mathbb{T} = \mathbb{R}/2\mathbb{Z}$ where we discretize the whole domain $\Omega \times \mathbb{R}^2$ with mesh size $\Delta x = 0.02$. We choose the spatial dimension, coupling strength and communication weight as follows:

$$d = 2, \quad \kappa = 1, \quad \phi \equiv 1.$$

We prepared the initial datum whose spatial density $\rho_0(x) := \int_{\mathbb{R}^2} f_0(x, v)\, dv$ is a uniform distribution inside the box $[0.24, 0.76] \times [-0.76, -0.24]$, and the velocity density $\xi_0(v) := \int_\Omega f_0(x, v)\, dx$ is also a uniform distribution inside the box $[0.24, 0.76] \times [0.24, 0.76]$ so that $f_0(x, v) = \rho_0(x)\xi_0(v)$ whose total mass is normalized to 1 (see Fig. 7). It shows that the ensemble of particles will collide against the right boundary, $x^1 = 1$, and then specularly reflected into the domain.

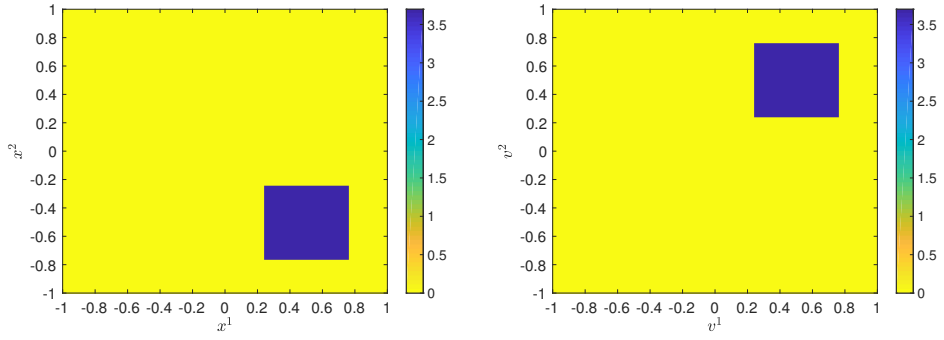

(a) Initial spatial density (b) Initial velocity density

FIG. 7. *Initial distribution for the kinetic model*

Fig. 8 plots the temporal evolution of the spatial density for the kinetic C-S model with the original flocking force. The velocity density is plotted in Fig. 9. The ensemble of particles aggregates in the x^1-direction, and we observe that the v^1-components of the velocities have tendencies to decay, and the v^1- and v^2-components of the velocities asymptotically become concentrated on a single value. Note that the velocities become much slower after the collision. The original flocking model makes the densities gather near the boundary, which is consistent with the particle dynamics in Fig. 2.

Fig. 10 and Fig. 11 show the results for the kinetic model with the flow-directional flocking forces, which differs significantly from Fig. 8 and Fig. 9. The results of Fig. 10 and Fig. 11 are consistent with the particle dynamics in Fig. 3. The support of the v^2-component of velocities becomes narrower and tends to shrink to a single value, while the density on the v^1-component keeps its support. This indicates that the flow-directional flocking on the x^2-direction emerges.

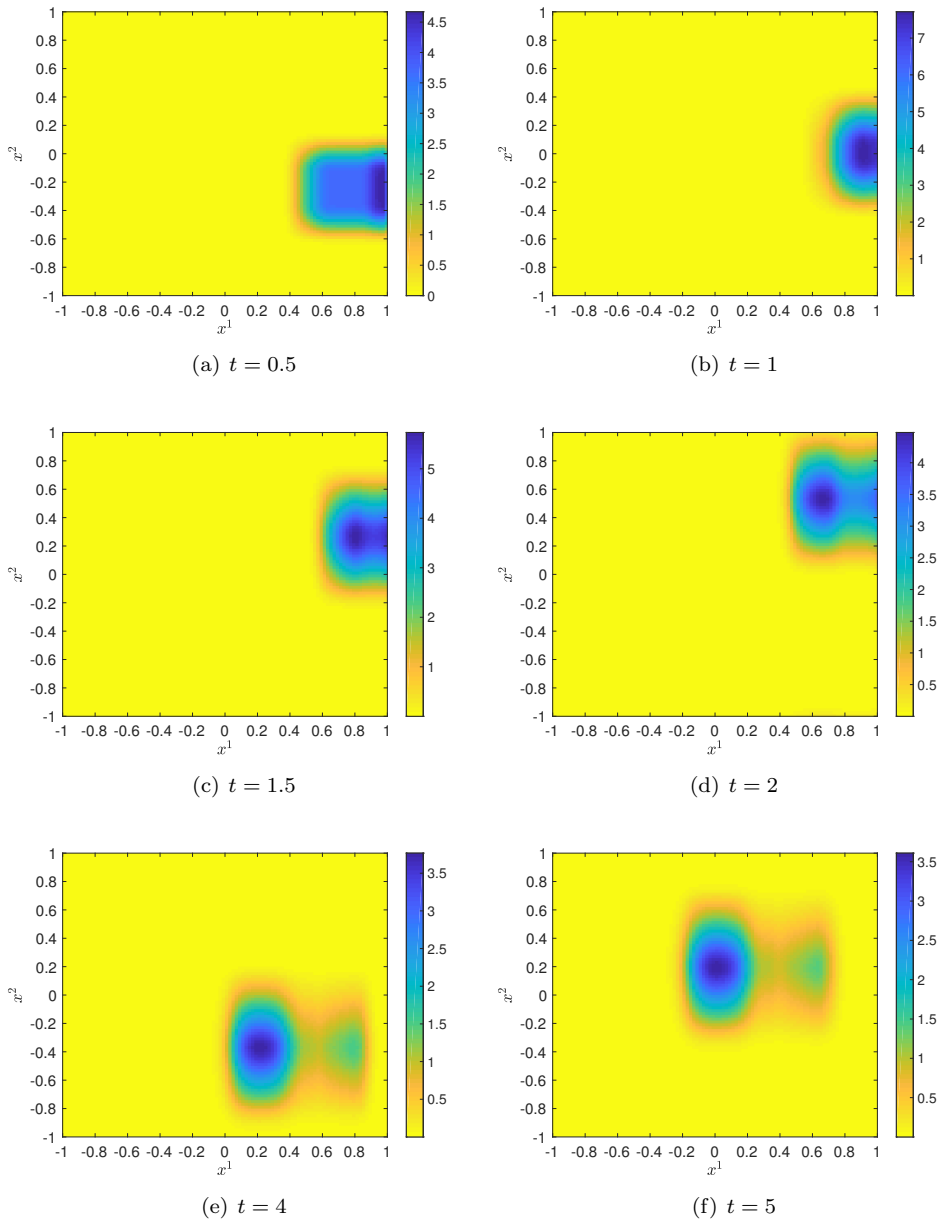

(a) $t = 0.5$ (b) $t = 1$

(c) $t = 1.5$ (d) $t = 2$

(e) $t = 4$ (f) $t = 5$

FIG. 8. *Temporal evolution of the spatial density for the original kinetic C-S model*

7. Conclusion. In this paper, we have studied the modified Cucker-Smale model in a cylindrical domain with a specular reflection boundary condition. In the case of the original flocking force, quite a large portion of C-S ensemble sticks to the boundary, as it can be seen in numerical simulations. To avoid this undesired phenomenon, namely "sticky aggregation near the boundary", we proposed a modified model with the flow-directional flocking force. We only allow the flocking force along the direction

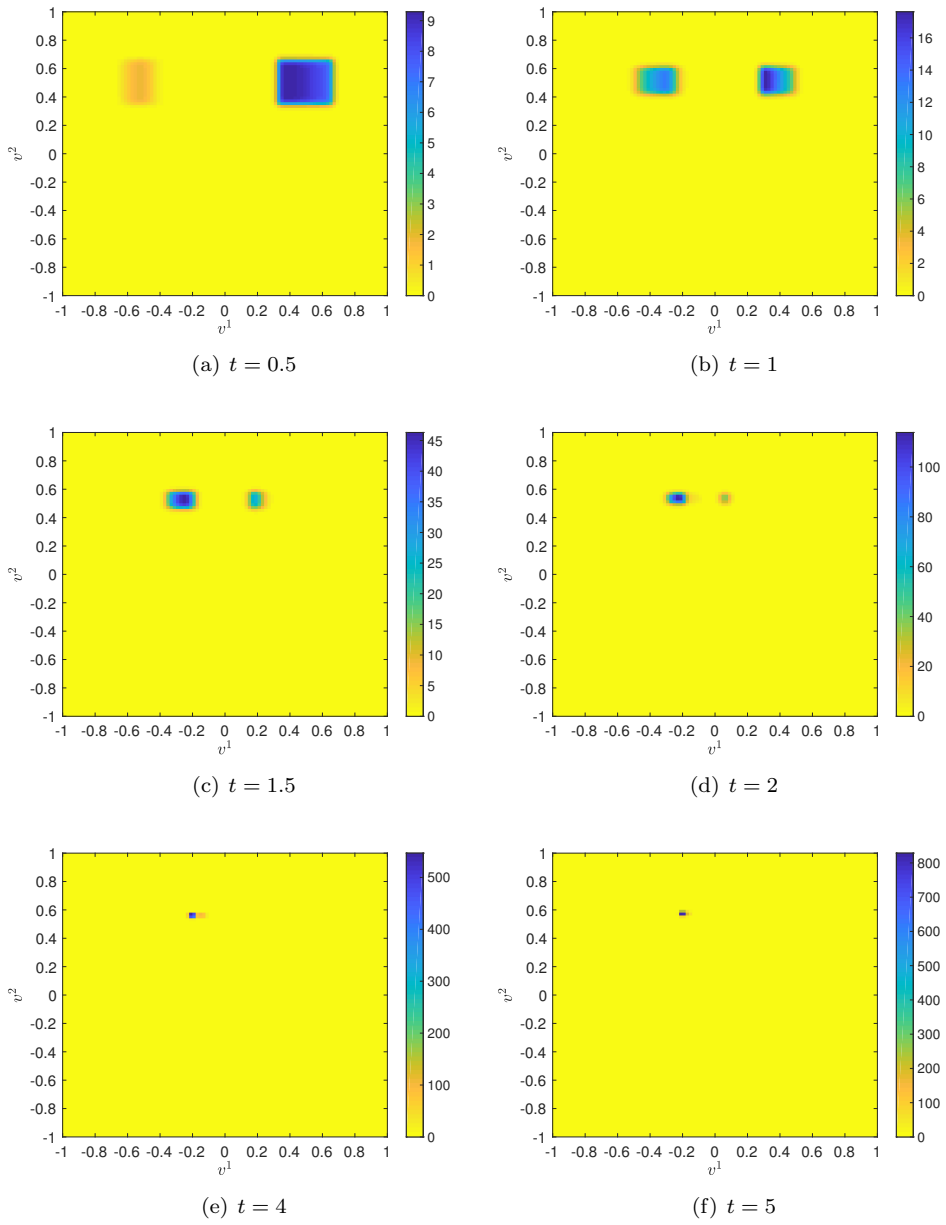

(a) $t = 0.5$ (b) $t = 1$

(c) $t = 1.5$ (d) $t = 2$

(e) $t = 4$ (f) $t = 5$

FIG. 9. *Temporal evolution of the velocity density for the original kinetic C-S model*

of the flow and turn off the force which is normal to the boundary. In this framework, we are able to show the emergence of flow-directional flocking along the flow direction. Moreover, we have developed a mesoscopic approach for this flow-directional flocking model, and provide the well-posedness of the classical solution to the kinetic model. Considering possible applications, it is a starting point of the interacting flocking particles along the domain with physical boundaries, such as a blood vessel or water

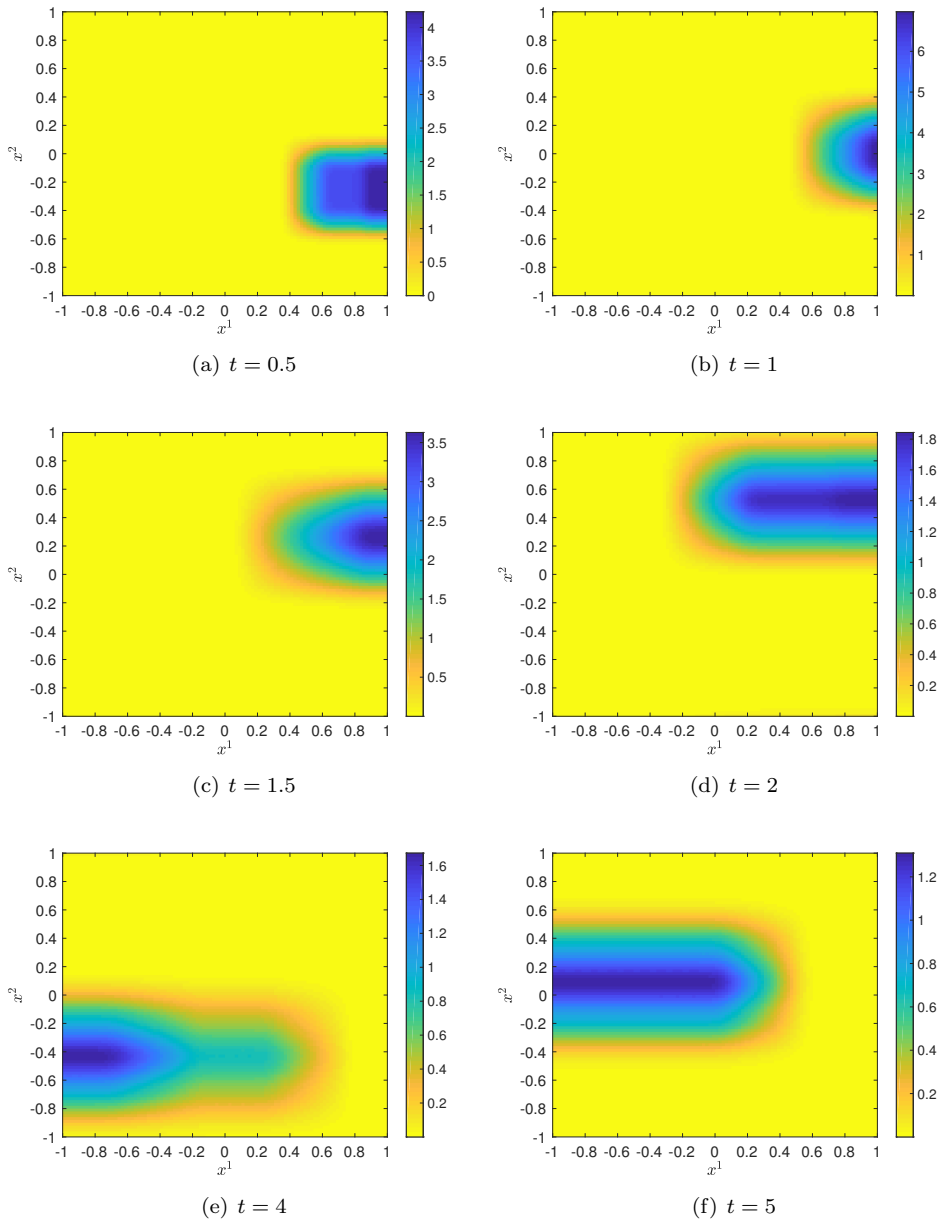

FIG. 10. *Spatial density for the kinetic C-S model with the flow-directional flocking force*

pipe. In this point of view, the coupling of the kinetic C-S model with the Navier-Stokes equation in the bounded domain, both specular or elastic boundary condition, can be a natural generalization of the kinetic model proposed in this paper. We leave these interesting problems for a future work.

Acknowledgement. The work of H.-O. Bae is partially supported by NRF grant (NRF-2018R1D1A1A09082848). The work of S.-Y. Ha is supported by the Samsung

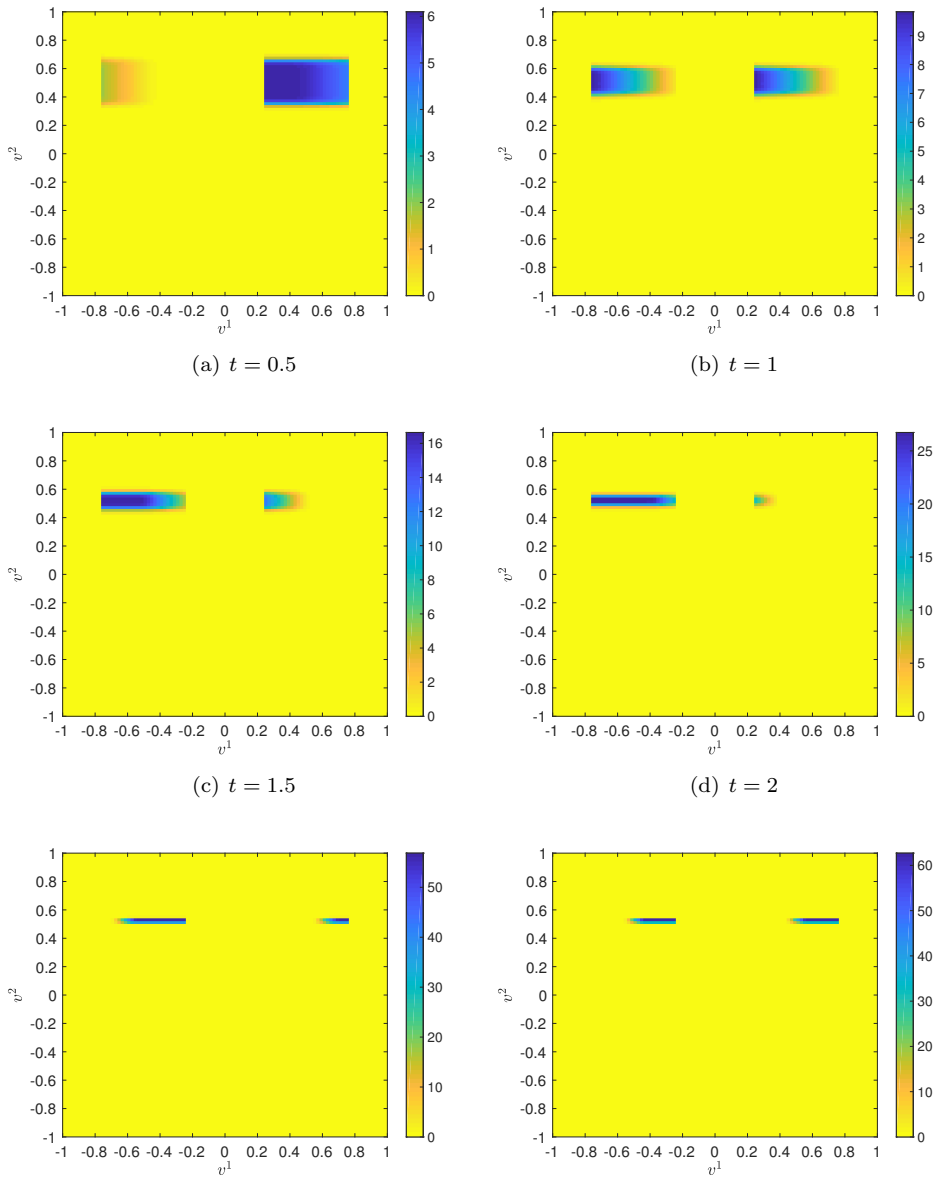

(a) $t = 0.5$ (b) $t = 1$

(c) $t = 1.5$ (d) $t = 2$

(e) $t = 4$ (f) $t = 5$

FIG. 11. *Velocity density for the kinetic C-S model with the flow-directional flocking force*

Science and Technology Foundation under Project Number SSTF-BA1401-03. The work of J. Kim is supported by the German Research Foundation under Project Number IRTG 2235. The work of D. Ko is supported by ERC-2015-AdG-694126-DyCon from the European Research Council, under the European Union's Horizon 2020 Research and Innovation Programme and by CNCS-UEFISCDI Grant No. PN-III-P4-ID-PCE-2016-0035. The work of S.-I. Sohn is partially supported by NRF

grant (NRF-2018R1A2B6002164).

REFERENCES

[1] Ahn, S. and Ha, S.-Y.: *Stochastic flocking dynamics of the Cucker-Smale model with multiplicative white noises.* J. Math. Phys. **51** (2010), 103301.

[2] Armbruster, D., Motsch, S. and Thatcher, A.: *Swarming in bounded domains.* Phys. D **344** (2017), 58–67.

[3] Bae, H.-O., Choi, Y.-P., Ha, S.-Y. and Kang, M.-J.: *Asymptotic flocking dynamics of Cucker-Smale particles immersed in compressible fluids.* Discrete Contin. Dyn. Syst. **34** (2014), 4419–4458.

[4] Bae, H.-O., Choi, Y.-P., Ha, S.-Y. and Kang, M.-J.: *Time-asymptotic interaction of flocking particles and incompressible viscous fluid.* Nonlinearity **25** (2012), 1155–1177.

[5] Bellomo, N. and Ha, S.-Y.: *A quest toward a mathematical theory of the dynamics of swarms.* Math. Models Methods Appl. Sci. **27** (2017), 745–770.

[6] Bertozzi, A. L., von Brecht, J., Sun, H., Kolokolnikov, T. and Uminsky, D.: *Ring patterns and their bifurcations in a nonlocal model of biological swarms.* Commun. Math. Sci. **13** (2015), 955–985.

[7] Bolley, F., Canizo, J. A. and Carrillo, J. A.: *Stochastic mean-field limit: non-Lipschitz forces and swarming.* Math. Models Methods Appl. Sci. **21** (2011), 2179–2210.

[8] Canizo, J. A., Carrillo, J. A. and Rosado, J.: *A well-posedness theory in measures for some kinetic models of collective motion.* Math. Models Methods Appl. Sci. **21** (2011), 515–539.

[9] Carrillo, J. A., D' Orsogna, M. R. and Panferov, V.: *Double milling in self-propelled swarms from kinetic theory.* Kinet. Relat. Models **2** (2009), 363–378.

[10] Carrillo, J. A., Fornasier, M., Rosado, J. and Toscani, G.: *Asymptotic flocking dynamics for the kinetic Cucker-Smale model.* SIAM J. Math. Anal. **42** (2010), 218–236.

[11] Cho, J., Ha, S.-Y., Huang, F., Jin, C. and Ko, D.: *Emergence of bi-cluster flocking for the Cucker-Smale model.* Math. Models Methods Appl. Sci. **26** (2016), 1191–1218.

[12] Choi, Y.-P., Ha, S.-Y. and Li, Z.: *Emergent dynamics of the Cucker-Smale flocking model and its variants.* In N. Bellomo, P. Degond and E. Tadmor (Eds.), Active Particles Vol. 1. Advances in theory, models and applications, 299-331, Model. Simul. Sci. Eng. Technol., Birkhäuser-Springer, Cham, (2017).

[13] Chuang, Y.-L., Huang, Y. R., D'Orsogna, M. R. and Bertozzi, A. L.: *Multi-vehicle flocking: scalability of cooperative control algorithms using pairwise potentials*, Proceedings 2007 IEEE International Conference on Robotics and Automation, Roma, (2007), 2292–2299.

[14] Cucker, F. and Smale, S.: *On the mathematics of emergence.* Japan. J. Math. **2** (2007), 197–227.

[15] Cucker, F. and Smale, S.: *Emergent behavior in flocks.* IEEE Trans. Automat. Control **52** (2007), 852–862.

[16] Degond, P. and Motsch, S.: *Macroscopic limit of self-driven particles with orientation interaction.* C. R. Acad. Sci. Paris, Ser. I **345** (2007), 555–560.

[17] Degond, P. and Motsch, S.: *Large-scale dynamics of the persistent Turing Walker model of fish behavior.* J. Stat. Phys. **131** (2008), 989–1022.

[18] Degond, P. and Motsch, S.: *Continuum limit of self-driven particles with orientation interaction.* Math. Models Methods Appl. Sci. **18** (2008), 1193–1215.

[19] Fornasier, M., Haskovec, J. and Toscani, G.: *Fluid dynamic description of flocking via Povzner-Boltzmann equation.* Phys. D **240** (2011), 21–31.

[20] Guo, Y.: *Regularity for the Vlasov equations in a half-space.* Indiana U. Math. J. **43**, (1994), 255–320.

[21] Ha, S.-Y., Kwon, B. and Kang, M.-J.: *Emergent dynamics for the hydrodynamic Cucker-Smale system in a moving domain.* SIAM. J. Math. Anal. **47** (2015), 3813–3831.

[22] Ha, S.-Y., Kwon, B. and Kang, M.-J.: *A hydrodynamic model for the interaction of Cucker-Smale particles and incompressible fluid.* Math. Models Methods Appl. Sci. **24** (2014), 2311–2359.

[23] Ha, S.-Y., Park, J. and Zhang, X.: *A first-order reduction of the Cucker-Smale model on the real line and its clustering dynamics.* Commun. Math. Sci. **16** (2018), 1907–1931.

[24] Ha, S.-Y., Kim, J., Park, J. and Zhang, X.: *Complete cluster predictability of the Cucker-Smale flocking model on the line.* Arch. Rational Mech. Anal. **231** (2019), 319–365.

[25] Ha, S.-Y., Ko, D. and Zhang, Y.: *Critical coupling strength of the Cucker-Smale model for flocking.* Math. Models Methods Appl. Sci. **27** (2017), 1051–1087.

[26] Ha, S.-Y., Kim, J. and Zhang, X.: *Uniform stability of the Cucker-Smale model and its appli-*

cation to the mean-field limit. Kinet. Relat. Models **11** (2018), 1157–1181.
[27] Ha, S.-Y., Lee, K. and Levy, D.: *Emergence of time-asymptotic flocking in a stochastic Cucker-Smale system.* Commun. Math. Sci. **7** (2009), 453–469.
[28] Ha, S.-Y. and Liu, J.-G.: *A simple proof of Cucker-Smale flocking dynamics and mean field limit.* Commun. Math. Sci. **7** (2009), 297–325.
[29] Ha, S.-Y. and Tadmor, E.:*From particle to kinetic and hydrodynamic description of flocking.* Kinet. Relat. Models **1** (2008), 415–435.
[30] Kuramoto, Y.: *International symposium on mathematical problems in mathematical physics.* Lecture Notes Theor. Phys. **30** (1975), 420.
[31] Leonard, N. E., Paley, D. A., Lekien, F., Sepulchre, D. Fratantoni, D. M. and Davis, R. E.: *Collective motion, sensor networks and ocean sampling.* Proc. IEEE **95** (2007), 48–74.
[32] Li, Z. and Xue, X.: *Cucker-Smale flocking under rooted leadership with fixed and switching topologies.* SIAM J. Appl. Math. **70** (2010), 3156–3174.
[33] Motsch, S. and Tadmor, E.: *Heterophilious dynamics enhances consensus.* SIAM Rev. **56** (2014), 577–621.
[34] Motsch, S. and Tadmor, E.: *A new model for self-organized dynamics and its flocking behavior.* J. Stat. Phys. **144** (2011), 923–947.
[35] Perea, L., Elosegui, P. and Gómez, G.: *Extension of the Cucker-Smale control law to space flight formation.* J. Guid. Control Dyn. **32** (2009), 526–536.
[36] Paley, D. A., Leonard, N. E., Sepulchre, R., Grunbaum, D. and Parrish, J. K.: *Oscillator models and collective motion.* IEEE Control Syst. Mag. **27** (2007), 89–105.
[37] Park, J., Kim, H. and Ha, S.-Y.: *Cucker-Smale flocking with inter-particle bonding forces.* IEEE Trans. Autom. Control **55** (2010), 2617–2623.
[38] Poyato, D. and Soler, J.: *Euler-type equations and commutators in singular and hyperbolic limits of kinetic Cucker-Smale models.* Math. Models Methods Appl. Sci. **6** (2017),1089–1152.
[39] Shen, J.: *Cucker-Smale flocking under hierarchical leadership.* SIAM J. Appl. Math. **68** (2007), 694–719.
[40] Toner, J. and Tu, Y.: *Flocks, herds, and schools: A quantitative theory of flocking.* Phys. Rev. E **58** (1998), 4828–4858.
[41] Topaz, C. M. and Bertozzi, A. L.: *Swarming patterns in a two-dimensional kinematic model for biological groups.* SIAM J. Appl. Math. **65** (2004), 152–174.
[42] Vicsek, T., Czirók, A., Ben-Jacob, E., Cohen, I. and Schochet, O.: *Novel type of phase transition in a system of self-driven particles.* Phys. Rev. Lett. **75** (1995), 1226–1229.
[43] Winfree, A. T.: *Biological rhythms and the behavior of populations of coupled oscillators.* J. Theor. Biol. **16** (1967), 15–42.